Cellular and behavioral functions of *Arl8b* gene revealed by targeted genome editing

Oda, Naoko

Doctor of Philosophy

Department of Genetics

School of Life Science

The Graduate University for Advanced Studies,

SOKENDAI

CONTENTS

ABSTRACT

ADP-ribosylation factor-like GTPase 8b (Arl8b) is a small GTPase which is primarily localized to lysosomes. Arl8b is known to be a key regulator for lysosome positioning. In mammalian cultured cell lines, Arl8b knockdown and overexpression induced the distribution of lysosomes in the perinuclear area and the cell peripheral area, respectively. Arl8b-mediated lysosomal positioning is closely related to nutrient state-dependent autophagy. As these previous studies have been conducted only on particular cell lines, we do not know whether the phenotypic effects of Arl8b in lysosomal functions are general in primary cells. In addition, *Arl8b* gene has been previously identified as one of the candidate genes underlying a variation in locomotor activity between a laboratory strain C57BL/6J (B6) and a wild-derived mouse strain MSM/MS (MSM). Although previous studies using Arl8b knockout mice showed that Arl8b is important for survival, degradation of maternal protein, and embryonic development, the functions of Arl8b in mouse behavior are still unknown.

In chapter 1, I examined the roles of Arl8b in lysosomal positioning in primary cells, mouse embryonic fibroblasts (MEFs). Using the CRISPR-Cas9 gene editing technique, I generated four types of *Arl8b* gene-edited mutant mouse: *Arl8b* gene knockout (*Arl8b*-KO), a mutant that has a 9-base pair deletion in the coding region of *Arl8b* gene ($Arl8b^{\Delta 9}$), GTP-bound form mutant ($Arl8b^{Q75L}$), and GDP-bound form mutant ($Arl8b^{T34N}$). $Arl8b^{\Delta 9}$ mutant was obtained by chance and its three amino acids deletion was located near an effector domain that interacts with motor proteins. First, I investigated whether lysosomal positioning is changed depending on nutritional states. In MEFs from wild-type (WT) mice, fetal bovine

serum starvation induced perinuclear clustering of lysosomes whereas nutritional recovery restored lysosome distribution to the cell periphery. Next, comparison among MEFs from the four types of Arl8b mutant and WT mice showed that lysosomal positioning was not different among genotypes under normal condition or starvation. However, a delay of a response to nutritional recovery was observed in MEFs from *Arl8b*$^{\Delta 9/\Delta 9}$ and *Arl8b*$^{T34N/T34N}$ mice compared to the WT MEFs, while the *Arl8b*$^{Q75L/Q75L}$ MEFs were similar to the WT MEFs. This suggests that lysosome positioning in response to nutrient recovery requires Arl8b function. Also, the sequence of the three amino acids deleted in *Arl8b*$^{\Delta 9}$ mutants may be important for proper Arl8b functions although these three amino acids are not located in GTP-binding domains.

In chapter 2, I investigated behavioral effects of Arl8b by using the *Arl8b* gene-edited mice. First, I examined whether the expression level of *Arl8b* gene is different between MSM and B6. MSM, which shows higher home-cage activity than B6, had higher expression levels of *Arl8b* gene in the striatum and cerebellum than B6. Next, before performing behavioral analyses, I checked the genotypes of the embryos and the newborn mice and found that homozygotes for *Arl8b*-KO, *Arl8b*$^{\Delta 9}$ and *Arl8b*^{T34N} died around birth, suggesting that Arl8b in its GTP-bound form is required for perinatal survival. Finally, behavioral tests of the Arl8b mutants were performed to measure the locomotor activity and anxiety-related behaviors. *Arl8b*$^{+/-}$ and *Arl8b*$^{Q75L/Q75L}$ did not show any difference from their WT littermates in any measurements. *Arl8b*$^{+/\Delta 9}$ mouse showed higher activity in the early phase of the dark period in the home-cage activity test. Also, *Arl8b*$^{+/\Delta 9}$ mouse showed significantly higher locomotor activity than WT in the open-field test and the light and dark box test. No statistically significant difference was detected

between *Arl8b*$^{+/T34N}$ mice and their WT littermates, but there was a tendency of *Arl8b*$^{+/T34N}$ mice increasing their locomotion activity in the open-field test.

In conclusion, I generated *Arl8b* gene-edited mutant mice and found that Arl8b function is important for lysosome positioning in response to the recovery of nutrition in primary cells. The three amino acids that are located near the effector domain may be important for Arl8b functions. Finally, my behavioral observations demonstrated that Arl8b might be an important regulator for the locomotor activity.

CHAPTER 1

Lysosomal positioning in Arl8b mutant MEF cells

1.1 INTRODUCTION

ADP-ribosylation factor-like GTPase 8b (Arl8b) is a member of the Arf family of small GTP-binding proteins and highly conserved from protozoans to metazoans as well as in plants (Li et al. 2004; Kahn et al. 2006; Khatter et al. 2015). Arl8 contains two paralogs, Arl8a and Arl8b, which share 91% amino acid identity in vertebrates (Hofmann and Munro. 2006). Arl8b consists of 186 amino acids and has a molecular weight of approximately 22kDa (Okai et al. 2004; Kahn et al. 2006). Arl8b protein contains an N-terminally acetylated amphipathic helix, a putative effector domain, and well-conserved GTP-binding domains (G1-G5) (Okai et al. 2004; Hofmann and Munro. 2006). Arl8b has been found to primarily localize to lysosomes and have an essential role in lysosome positioning (Hofmann and Munro. 2006). Arl8b regulates lysosomal motility along microtubules with kinesins, the Arl8b effector SifA and kinesin-interacting protein (SKIP, also known as PLEKHM2), and BLOC-one-related (BORC) complex (Boucrot et al. 2005; Bagshaw et al. 2006; Hofmann and Munro. 2006; Rosa-Ferreira and Munro. 2011; Pu et al. 2015).

Previous studies using cell lines have demonstrated the importance of Arl8b for lysosome localization. A study using COS cells indicated that N-terminal acetylation of Arl8b is important for its lysosomal localization (Hofmann and Munro. 2006). Also, a previous study showed that cells with knockdown of Arl8b showed perinuclear clustering of lysosome in several cell lines (Garg et al. 2011; Korolchuk et al. 2011). Overexpression of Arl8b increased

accumulation of lysosomes at the cell periphery of cells. (Bagshaw et al. 2006; Hofmann and Munro. 2006). Furthermore, it has been revealed that the GTPase activity of Arl8b affects lysosome motility. In normal rat kidney epithelial (NRK) cells expressing Arl8b, lysosomes moved more frequently and over longer distances. Similar tendency was observed in NRK cells expressing Arl8b-Q75L, which is a GTP-bound form mutant (Hofmann and Munro. 2006).

Arl8b-mediated lysosomal positioning was reported to be involved in lysosome functions including metabolic signaling and autophagy (Korolchuk et al. 2011). Previous studies showed that lysosomes have two spatially distinct subsets: a relatively static perinuclear subset near the microtubule-organizing center (MTOC) and a highly dynamic peripheral subset, and these two subsets have different biological functions (Johnson et al. 2016; Jongsma et al. 2016). For example, perinuclear lysosomes fuse with autophagosomes to generate autolysosomes. In contrast, peripheral lysosomes activate mammalian target of rapamycin complex 1 (mTORC1) signaling (Encarnação et al. 2016; Korolchuk et al. 2011; Nakamura et al. 2017). mTORC1 is a serine/threonine kinase, which promotes anabolic responses including protein synthesis while inhibiting the catabolic process of autophagy (Caron and Laplante. 2015; Encarnação et al. 2016; Saxton and Sabatini. 2017). In normal cells, it has been known that mTORC1 inactivity and increase of autophagic activity suppress cell growth and support cell survival (Carroll and Korolchuk. 2018). Under nutrient sufficient status, lysosomes are transported to the cell peripheral region and activates mTORC1 signaling (Figure 1A). On the other hand, a nutrient depletion interrupts the centrifugal movement of lysosomes along microtubules, leading to a reduced activity of mTORC1 (Korolchuk et al. 2011). Simultaneously, autophagy-related substrates including UNC51-like kinase 1 (ULK1) and the transcription factor EB (TFEB) are dephosphorylated, resulting in promoting autophagy (Figure 1B) (Itakura and Mizushima. 2010; Palmieri et al. 2011;

Settembre et al. 2012; Martina et al. 2012). However, a replenishment of amino acids after starvation can lead to redistribution of lysosomes to the cell periphery (Berger et al. 2006; Hofman and Munro. 2006; Korolchuk et al. 2011). In HeLa cells, knockdown of Arl8b leads to perinuclear clustering of lysosome, diminished mTORC1 activity, and increased autophagic activity (Korolchuk et al. 2011). In contrast, distribution of lysosomes to the cell periphery by overexpression of Arl8b increased mTORC1 activity in HeLa cells (Korolchuk et al. 2011).

Although these previous studies revealed the importance of Arl8b on lysosomal positioning, all studies were performed in cell lines. Cell lines are generally highly proliferative and easy to be cultured, but display genetic and phenotypic differences from their tissue of origin because most cell lines have been maintained in the lab for long time, often derived from cancer cells, and adapted to the two-dimensional culture environment (Alge et al. 2006; Pan et al. 2009). On the other hand, primary cells are isolated directly from tissues, so they are likely to retain a normal cell morphology and functional characteristics of their tissue of origin (Alge et al. 2006; Pan et al. 2009). It remains unclear whether the activity of Arl8b is required for lysosomal positioning in the primary cells.

In this chapter, I investigated the function of Arl8b using a primary cell, mouse embryonic fibroblasts (MEFs). The MEFs are derived from 12.5 to 15.5 days post coitum (dpc) after removing the head and viscera region and used for studying many biological properties such as cell cycle regulation, senescence, apoptosis (Lowe et al. 1994; Steinman et al. 2004; Sun et al. 2007). First, I generated four types of *Arl8b* mutants: *Arl8b*-knockout (KO), three amino acid deleted mutant $Arl8b^{\Delta 9}$, Arl8b GTP-binding form mutant $Arl8b^{Q75L}$, Arl8b GDP-binding form mutant $Arl8b^{T34N}$. $Arl8b^{\Delta 9}$ mutant was obtained by chance and deficient in three amino acids between GTP binding domains G1 and G2. Next, since mTORC1 signaling affects cell growth, I monitored the replicative capacity of MEF cells derived from the *Arl8b* gene-edited

mutants. It has been known that mouse fibroblasts undergo the replicative senescence under the standard culture conditions due to DNA damage caused by an oxidative stress (Parrinello et al. 2003). Therefore, I compared the replicative capacity among genotypes by using a 3T3 serial passage protocol (see below). Third, I investigated whether the Arl8b mutation affects lysosome motility under the cellular nutritional change. I examined lysosome distribution with a normal, starvation and recovery treatment in MEFs of the *Arl8b* gene-edited mice.

1.1 MATERIAL AND METHODS

Animals

All the mouse strains were maintained at the National Institute of Genetics (NIG) (Mishima, Japan) under a 12 h light / dark cycle (light from 6:00 to 18:00) in a temperature control room (23 ± 2 ℃). The mice were weaned from 25 to 31days of age and housed in same sex littermates in standard sized plastic cages on wood chips. Food and water were available ad libitum. Mice were maintained according to NIG guidelines, and all procedures were carried out with approval by our institutional animal care and use committee.

Genome editing

To design specific and efficient guide RNA sequences for the CRISPR-Cas9 gene editing, the CRISPR Design Tool (Ran et al. 2013), Benchling (Pellegrini, R. 2016), and CRISPOR (Haeussler et al. 2016) were used. Using the pX330 vector (#42230, Addgene, Watertown, MA, USA), template DNAs for *in vitro* transcription of the guide RNAs were amplified by PCR using Tks Gflex DNA polymerase (R060, Takara) with a primer containing the sequences of the T7 promoter and the target site. The primers were designed to mimic the previously reported optimized sgRNA sequence (Chen et al. 2013). The guide RNAs were synthesized with the MEGAshortscript™ T7 Transcription Kit (AM1354, Thermo Fisher Scientific).

For a deletion of *Arl8b* coding sequence, the guide RNA (50 ng / μl) and Cas9 protein (1074181, Integrated DNA Technologies, Coralville, IA, USA) (50 ng / μl) were microinjected into the pronuclei of fertilized B6 oocytes with the oligo DNA (50 ng / μl or 100 ng / μl) that was designed to join both sides of the inserted site (Table 1). *Arl8b*-KO and *Arl8b*$^{\Delta 9}$ mice were generated by using the same guide RNA and oligo DNA (Table 1). As there are previous reports on the GTP-bound form (Arl8b-Q75L) and GDP-bound form (Arl8b-T34N) (Hofmann and Munro, 2006; Okai et al., 2004; Garg et al., 2011), I designed the oligo DNA that contains the target mutations for generating the GTP-bound form and GDP-bound mutant of Arl8b (Table1). For genotyping of the *Arl8b*^{Q75L} mice by using restriction enzyme, I designed the oligo DNA that can induce a silent mutation for changing the restriction site as well as a targeted point mutation. The guide RNA (50 ng/μl), Cas9 protein (50 ng/μl) and the oligo DNA (50 ng/μl or 100 ng/μl) were microinjected into the pronuclei of fertilized B6 oocytes.

The injected zygotes were transferred into pseudopregnant female ICR mice. The pups were genotyped by genomic PCR. In case of GTP-bound or GDP-bound form mutants, a restriction enzyme treatment was performed after genomic PCR. A correctly targeted allele was also confirmed by direct sequencing of the PCR product. After confirming the correctly targeted allele, a founder was crossed with B6 and F_1 mice were checked whether they have the mutant allele by genomic PCR and sequencing.

Genomic PCR

Genomic DNA was extracted from mouse ears or tails. TE buffer was added into tubes which contained ears or tails. The tubes were heated for 5 mins at 95℃. After heating,

Proteinase K was added, and the tubes were incubated at 55℃ overnight. Inactivation of Proteinase K was performed by heating the samples for 5 minutes at 95℃. The extracted DNA was amplified by PCR using Tks Gflex DNA polymerase with primers. The sequence and the genomic positions of primers used for genomic PCR are listed in Table 1. Genotyping of the *Arl8b*^{Q75L} or *Arl8b*^{T34N} mice were performed by PCR amplification following *Nla*IV or *Xmn*I enzyme treatment respectively.

Western blotting

To check Arl8b protein expression by Western blotting, E18.5 embryonic brains were used. Embryos derived from crossing heterozygous mice of each *Arl8b*$^{+/-}$ or *Arl8b*$^{+/\Delta 9}$ at embryonic day 18.5 (E18.5). Protein expression was compared between littermates. Western blotting was performed using anti-Gapdh (1:10000, clone 6C5, ORIGENE), and anti-Arl8 (1:400, provided by Dr. Kenji Kontani (Meiji Pharmaceutical University, Tokyo, Japan)). HRP-conjugated secondary antibodies were used: anti-mouse IgG (1:10000, 170-6516, BIORAD), anti-rabbit IgG (1:10000, 170-5046, BIORAD).

Mouse Embryonic fibroblasts (MEFs) cell isolation

Mouse embryonic fibroblasts (MEFs) were prepared as follows. Embryos derived from crossing heterozygous mice of each *Arl8b* mutant at E15.5. Head and internal organs were removed. The remaining body tissue of embryo was minced into small fragments. After

adding 0.1% trypsin-EDTA (20ml / 4~5 embryos), minced tissues were transferred to a 50 ml conical tube for enzymatic digestion for 20 minutes with shaking. After pipetting up and down several times to disaggregate the tissue, another 0.1% trypsin-EDTA (20ml / 4~5 embryos) were added with shaking for another 20 minutes. The lysates were transferred to a tube that contains Dulbecco's modified Eagle's medium (DMEM) (11965-092, Thermo Fisher Scientific, Gibco) with 20% Fetal bovine serum (FBS), and cells were dispersed by pipetting up and down in the culture medium. Then, the supernatant was transferred into new 50 ml tube and centrifuged at 1,000 rpm for 5 minutes. Dissociated cells were cultured in the complete medium (DMEM supplemented with 10% FBS, 1% penicillin and streptomycin) at 37℃ under 5% CO_2. The medium was changed on the following day. After reaching at 80% confluent, cells were collected and cryopreserved by using CELLBANKER 1 plus (CB023, Takara).

MEF culturing and 3T3 serial passaging

MEFs were cultured in DMEM supplemented with 10% FBS and 1% penicillin and streptomycin. For replicative senescence experiments, a 3T3 protocol was followed by counting cells and reseeding 1 x 10^6 cells per 10 cm plate every 3 days (Chua et al. 2005). Two biological duplicates per genotype were assessed.

Starvation and recovery protocols

The starvation and recovery protocols in this study followed a method described in Korolchumk et al., 2011. P2 cells were plated at the density of 0.03 x 10^6 cells / well on coverslips (C015001, Matsunami Glass Ind., Ltd.) in 12-well plates (353043, Corning, Falcon) and grown in the complete medium at 37℃ under 5% CO_2 for one day. In this study, cells were divided into three groups; no treatment group, starvation group, and recovery group. On day 2, cells in the no treatment group were added 1 ml of fresh complete medium and grown for 24 h at 37℃ under 5% CO_2. In contrast, cells in the starvation group and the recovery group were washed briefly in 1 ml of serum-free DMEM (11965-092, Thermo Fisher Scientific, Gibco), the media was aspirated, and 1 ml of fresh serum-free DMEM was added and the cells were cultured for 24 hours at 37℃ under 5% CO_2. On day 3, cells in both the no treatment group and the starvation group were fixed with 4% paraformaldehyde (PFA) in PBS simultaneously. Cells in the recovery group were added 1 ml DMEM with extra x1 amino acids (MEM amino acids x50 liquid, 11130051, Gibco and L-glutamine x100 liquid, 25030081, Thermo Fisher Scientific, Gibco) at pH 7.0. To examine a change in lysosome distribution by the recovery treatment, cells in the recovery group were fixed by 4% paraformaldehyde (PFA) after 1 h, 3 h, 6 h and 12 h respectively. In these experiments, five genotypes were treated simultaneously. Three biological replicates were carried out in independent experiments in triplicate.

Immunofluorescence

After fixation with 4% PFA for 20 min, cells were washed with PBS and permeabilized with 0.1 % Triton X (168-11805, Wako) in PBS for 15 min. After washing with PBS, cells were blocked with 3% bovine serum albumin (01863-77, Nacalai tesque) in PBS. Cells on coverslips were incubated with anti-Lamp1 (1:500, ab25245, abcam) and anti-β-tublin (1:500, T4026, Sigma-Aldrich) overnight at 4℃. After washing two times with PBS, cells were incubated with anti-mouse IgG Alexa-488 (1:500, ab150133, Abcam), anti-rat IgG Alexa-555 (1:500, ab150154, Abcam), Alexa-647 Phalloidin and Hoechst 33342 (1:1000, 382065, Sigma-Aldrich, Calbiochem) for 90 min at room temperature in a darkroom. After washing three times with PBS, the coverslips were mounted with Fluoromount-G (0100-01, SouthernBiotech). In the immunofluorescence staining, experiments on five genotypes under all conditions were performed at once. Immunofluorescent images were captured using a confocal laser scanning microscope (FV-1000-D, Olympus, Japan).

Quantification of lysosomal distribution

For scoring lysosomal distribution, three 20x florescent images were analyzed per genotype per condition. Each image was captured from different coverslips which had cells derived from the same embryo under the same condition. Therefore, 9 images were obtained per genotype per condition (5 genotypes x 3 biological replicates x 3 images x 6 conditions = 270 images) (Figure 2). ROI manager in Image J was used for calculating a ratio of a whole cell body area to a lysosome-detected area as follows. At first, a whole cell body was encircled

manually according to the β-tublin-stained area: β-tublin is a cytoskeleton marker. Next, an area where Lamp-1 signal was detected was encircled manually. Each area was measured by ROI manager automatically and the ratio of the lysosome detected area divided by the whole cell body area in each cell was calculated. I confirmed that the value of the ratio is corresponding to the change of lysosome distribution. 20-50 cells were measured in each image. This quantification was performed blindly to the genotypes of the MEFs and conditions.

To see the ratio distribution, the number of cells per image were calculated by dividing the ratio into 10 groups: ratio < 0.1, 0.1 ≤ ratio < 0.2, 0.2 ≤ ratio < 0.3, 0.3 ≤ ratio < 0.4, 0.4 ≤ ratio < 0.5, 0.5 ≤ ratio < 0.6, 0.6 ≤ ratio < 0.7, 0.7 ≤ ratio < 0.8, 0.8 ≤ ratio < 0.9, 0.9 ≤ ratio. The percentages of cells in each group were calculated per image. Histogram was made by taking an average frequency of each group from 9 images (3 images x 3 embryos = 9 images). The average ratio of each genotype under each condition was calculated by taking an average from nine ratios (3 ratios x 3 embryos = 9 ratios). Additionally, cells were categorized into two types: perinuclear-dominant lysosomal pattern (cells with the ratio less than 0.4) and peripheral-dominant pattern (cells with the ratio more than 0.4).

Statistical analysis

Statistical significance was determined by analysis of variance (ANOVA) followed by Bonferroni / Dunnett test for multiple-comparison of body weight among genotypes and lysosomal positioning among conditions or genotypes. Differences were considered to be significant at $p < 0.05$. The calculations were performed using StatView 5.0 (SAS Institute Inc., USA).

1.3 RESULTS

Development of *Arl8b* gene-edited mice

To investigate the function of Arl8b in primary cells, I generated four kinds of *Arl8b* mutant (Figure 3A). GTP-bound form mutant (*Arl8b*^{Q75L}) and GDP-bound form mutant (*Arl8b*^{T34N}) had one amino acid substitution as shown in Figure 3B. *Arl8b*$^{\Delta 9}$ was obtained by chance and this had the deletion of three amino acids near the G2 sequence (Figure 3B). Genotyping of the *Arl8b*^{Q75L} or *Arl8b*^{T34N} mice were confirmed by PCR analyses and restriction enzyme treatment (Figure 3C). No protein expression of Arl8b in *Arl8b*-KO (*Arl8b*$^{-/-}$) was detected while the protein expression of Arl8b was detected in homozygous mice of *Arl8b*$^{\Delta 9}$ (*Arl8b*$^{\Delta 9/\Delta 9}$) (Figure 3D).

No clear difference in cell proliferation of MEFs among *Arl8b* gene-edited mutants

Since Arl8b-mediated lysosome positioning affects mTORC1 signaling which is involved in cell growth, I first examined the effect of Arl8b mutation on cell proliferation by using MEFs from *Arl8b*-KO and *Arl8b*$^{\Delta 9}$ embryos. I isolated MEFs from these mutant embryos at E15.5 and compared replicative senescence to serial passage in the *Arl8b*-KO cell line: *Arl8b*$^{+/+}$, *Arl8*$^{+/-}$ and *Arl8*$^{-/-}$ MEFs or in the *Arl8b*$^{\Delta 9}$ cell line: *Arl8b*$^{+/+}$, *Arl8b*$^{+/\Delta 9}$ and *Arl8b*$^{\Delta 9/\Delta 9}$ MEFs according to a 3T3 protocol (Figure 4). The cell proliferation gradually declined as the passage progresses in *Arl8b*$^{+/+}$, *Arl8*$^{+/-}$ and *Arl8*$^{-/-}$ MEFs as shown in Figure 4A. There was no obvious difference in cell proliferation among MEFs from *Arl8b*$^{+/+}$, *Arl8*$^{+/-}$ and *Arl8*$^{-/-}$. Figure

4B shows a cell proliferation change along passaging in the *Arl8b*$^{\Delta 9}$ cell line. Like *Arl8b*-KO cell line, replicative senescence occurred similarly among three genotypes (Figure 4B).

Redistribution of lysosome to the cell periphery after a nutritional recovery was delayed in *Arl8b* mutant MEFs

Next, I investigated whether Arl8b affects lysosome motility upon cellular nutritional change in MEFs. I first examined a starvation and a recovery protocol for WT MEF cells according to the previous study of HeLa cells (Figure 5A) (Korochuk et al. 2011). FBS starvation for 24 h increased the proportion of cells with predominantly perinuclear lysosomes (Figure 5B). Although a previous study of HeLa cells has reported that 30 min recovery treatment (adding amino acids together with FBS) after FBS starvation restored lysosome distribution (Korochuk et al. 2011), in my study of MEFs, even 1 h recovery treatment seemed not enough for the restoration of lysosomal distribution (Figure 5B). In WT MEFs, 6 h recovery treatment was required for the lysosomes to localize almost entirely to the cell body (Figure 5B). Next, to examine whether the *Arl8b* gene mutation affects lysosome distribution under nutritional conditions, I observed lysosome distribution of MEFs from the *Arl8b* gene-edited mutants at 6 conditions; no treatment, FBS starvation-treatment for 24 h, and recovery treatment for 1 h, 3 h, 6 h and 12 h (Figure 6). Lysosome distribution at 12 h recovery treatment was examined because the Arl8b mutations might change the duration of lysosomal redistribution to the cell periphery. I measured a whole cell body area and a lysosome detected area and calculated a ratio (lysosome detected area / whole cell body area) (Figure 7). A value of the ratio corresponded to lysosomal positioning within the cells

(Figure 8). The higher the value of the ratio was, the more widely lysosomes were distributed within the cell. After calculating the ratio of individual cells, I compared the ratio distribution, the average ratio and the pattern of lysosome distribution among MEFs from Arl8b mutants.

Arl8b$^{\Delta 9/\Delta 9}$ and Arl8b$^{T34N/T34N}$ showed a different peak distribution of the ratio after recovery

Figure 9 is the histogram showing the ratio value distribution of the 6 conditions: no treatment (A), FBS starvation for 24 h (B), FBS starvation and recovery treatment for 1 h (C), 3 h (D), 6 h (E), 12 h (F) in MEFs of control, *Arl8b*-KO, *Arl8b$^{\Delta 9/\Delta 9}$*, *Arl8b$^{Q75L/Q75L}$*, and *Arl8b$^{T34N/T34N}$*. In the control cells, a distribution's peak was located between 0.5 to 0.6 without any treatment (Figure 9A). However, after FBS starvation for 24 h, the distribution's peak was shifted to lower range of the value, 0.3-0.4, suggesting that the number of cells having perinuclear lysosomes increased after starvation (Figure 9B). The 1 h recovery treatment increased the proportion of cells showing the ratio of less than 0.3 and decreased the proportion of cells showing the ratio value of more than 0.5 compared to the starvation group (Figure 9C). After the 6h recovery treatment, the distribution's peak of the control was shifted to higher range of the value, 0.4-0.5 (Figure 9E). In the control cells, the distribution's peak returned to the original state in response to nutritional replenishment after starvation.

Under both the no treatment condition and the FBS starvation condition, all Arl8b mutant cells showed a similar distribution's peak to the control cells (Figure 9A and 9B). The *Arl8b*-KO cells showed the ratio within the range of 0.4-0.5 whereas other mutant cells showed a similar distribution's peak to the control cells (Figure 9A). After FBS starvation for 24 h, the distribution's peak of the *Arl8b$^{T34N/T34N}$* cells was ranging from 0.2-0.4, suggesting that a

greater number of the *Arl8b*$^{T34N/T34N}$ cells has predominantly perinuclear lysosomes (Figure 9B).

Compared to the control cell, the *Arl8b*$^{\Delta 9/\Delta 9}$ and the *Arl8b*$^{T34N/T34N}$ cells showed different peak distributions after the recovery treatment. Under the 1 h recovery treatment, the number of cells having the ratio value of less than 0.3 remarkably increased in the *Arl8b*$^{\Delta 9/\Delta 9}$ and *Arl8b*$^{T34N/T34N}$ cells. Even after the 3 h recovery treatment, the distribution's peak of the *Arl8b*$^{\Delta 9/\Delta 9}$ and *Arl8b*$^{T34N/T34N}$ cells remained in the range of 0.2-0.4 (Figure 9D). In contrast, the *Arl8b*$^{Q75L/Q75L}$ cells had a similar distribution's peak to the control cells under the 3 h recovery treatment (Figure 9D). The 6 h recovery treatment increased the population of the cells with the ratio value of more than 0.4 in the *Arl8b*$^{Q75L/Q75L}$ cells, which are similar to the control cells (Figure 9E). In contrast, a distribution's peak of the ratio of the *Arl8b*$^{\Delta 9/\Delta 9}$ and the *Arl8b*$^{T34N/T34N}$ cells still remained at a lower ratio value (Figure 9E). *Arl8b*-KO cells showed an intermediate phenotype between the control cell and the *Arl8b*$^{T34N/T34N}$ cells (Figure 9E). After the recovery treatment for 12 h, a distribution's peak of the *Arl8b*$^{Q75L/Q75L}$ cells were in the range of 0.4-0.5 whereas that of the *Arl8b*$^{\Delta 9/\Delta 9}$ and *Arl8b*$^{T34N/T34N}$ cells was in the range of 0.3-0.2 (Figure 9F). Taken together, the change of distribution's peak after recovery was delayed in the *Arl8b*$^{\Delta 9/\Delta 9}$ and *Arl8b*$^{T34N/T34N}$ cells.

The average ratios of lysosomal positions were significantly lower in Arl8b$^{\Delta 9/\Delta 9}$ *and Arl8b*$^{T34N/T34N}$ *than in the control after 1h and 3h recovery treatment*

Figure 10 indicates average ratios among genotypes in each condition. In the starvation condition, an average ratio of the control cells was higher than that of the *Arl8b*$^{T34N/T34N}$ cells,

but there was no significant difference (p = 0.0094, Bonferroni / Dunnett test). After 1 h recovery, the average ratio of the *Arl8b*$^{\Delta 9/\Delta 9}$ and *Arl8b*$^{T34N/T34N}$ cells was significantly smaller than the control cells (*Arl8b*$^{\Delta 9/\Delta 9}$ p = 0.0002, *Arl8b*$^{T34N/T34N}$ p = 0.0003, Bonferroni / Dunnett test). After the 3 h recovery treatment, the *Arl8b*-KO, *Arl8b*$^{\Delta 9/\Delta 9}$ and *Arl8b*$^{T34N/T34N}$ cells showed a significantly lower average ratio than the control cells (*Arl8b*-KO p = 0.0014, *Arl8b*$^{\Delta 9/\Delta 9}$ p = 0.0003, *Arl8b*$^{T34N/T34N}$ p = 0.0015, Bonferroni / Dunnett test). After the 6 h recovery treatment, the score of the average ratio of the *Arl8b*$^{T34N/T34N}$ cells was significantly lower than control (*Arl8b*$^{T34N/T34N}$ p = 0.0041, Bonferroni / Dunnett test). In the 12 h recovery treatment, the *Arl8b*$^{\Delta 9/\Delta 9}$ and *Arl8b*$^{T34N/T34N}$ cells has no difference from the control. The *Arl8b*$^{Q75L/Q75L}$ cells did not show any significant difference from the control in any treatment. These results suggest that the *Arl8b*$^{\Delta 9/\Delta 9}$ and *Arl8b*$^{T34N/T34N}$ cells showed more perinuclear lysosome distribution than the control.

Cells with predominantly peripheral lysosomes were significantly fewer in Arl8b$^{\Delta 9/\Delta 9}$ *and Arl8b*$^{T34N/T34N}$ *MEFs than in control after recovery*

To score lysosomal distribution, cells were categorized into two categories: perinuclear-dominant lysosomal pattern and peripheral-dominant lysosomal pattern. Because the analysis of histogram showed an apparent difference among genotypes at the ratio value of around 0.4 (Figure 9), cells with the ratio value of less than 0.4 was categorized as cells with perinuclear-dominant lysosomal pattern and cells with the ratio value of more than 0.4 as cells with peripheral-dominant lysosomal pattern. Without any treatment, more than 80% of cells showed peripheral-dominant lysosomal pattern in all genotypes (Figure 11). Figure 12

indicates representative images of each strain under each condition. Figure 13 shows the percentage of cells with predominantly peripheral lysosome distribution in each condition in the control (A), *Arl8*-KO (B), *Arl8b*$^{\Delta 9/\Delta 9}$ (C), *Arl8b*$^{Q75L/Q75L}$ (D) and *Arl8b*$^{T34N/T34N}$ cells (E). In the control cells, the proportion of the cells with predominantly peripheral lysosome was significantly decreased in the starvation treatment, 1 h recovery and 3 h recovery treatment (starvation $p < 0.0001$, 1 h recovery treatment $p < 0.0001$, 3 h recovery treatment $p < 0.0001$, Bonferroni / Dunnett test). After the 6 h recovery treatment, there was no significant difference from the no treatment, suggesting that the 6 h recovery treatment restored lysosomal distribution in the control cells (Figure 13A). On the other hand, the *Alr8b*-KO, *Arl8b*$^{\Delta 9/\Delta 9}$ and *Arl8b*$^{T34N/T34N}$ cells did not restore the lysosomal distribution even after the 6 h recovery treatment (Figure 13B, C and E). Like the control cells, a greater number of the *Arl8b*$^{Q75L/Q75L}$ cells with predominantly peripheral lysosome was increased after the 6 h recovery treatment (Figure 13D). Figure 14 shows a comparison among genotypes within the same condition. At the 1 h recovery treatment, the percentage of the control cells with predominantly peripheral lysosome was significantly higher than that of the *Arl8b*$^{\Delta 9/\Delta 9}$ and *Arl8b*$^{T34N/T34N}$ cells (*Arl8b*$^{\Delta 9/\Delta 9}$ $p < 0.0001$, *Arl8b*$^{T34N/T34N}$ $p = 0.002$, Bonferroni / Dunnett test). At the 3 h recovery treatment, a fewer number of the *Arl8b*$^{T34N/T34N}$ cells showed the predominantly peripheral lysosomal pattern than the control cells ($p = 0.017$, Bonferroni / Dunnett test). A greater number of the *Arl8b*$^{T34N/T34N}$ cells showed perinuclear-dominant lysosomal pattern than the control and *Arl8b*$^{Q75L/Q75L}$ cells (control versus *Arl8b*$^{T34N/T34N}$, $p = 0.0039$; *Arl8b*$^{Q75L/Q75L}$ versus *Arl8b*$^{T34N/T34N}$, $p = 0.0027$, Bonferroni / Dunnett test). These results suggest that the *Arl8b*$^{\Delta 9/\Delta 9}$ and *Arl8b*$^{T34N/T34N}$ cells may have severer defects in lysosome distribution responding to the cellular nutritional status.

1.4 DISCUSSION

In the present study, I examined the function of Arl8b in lysosomal positioning in MEF cells by generating *Arl8b* gene-edited mice by CRISPR/Cas9 gene editing technique. I generated four types of *Arl8b* gene-edited mutants: *Arl8b*-KO, *Arl8b*$^{\Delta 9}$, GTP-binding form mutant *Arl8b*^{Q75L} and GDP-binding form mutant *Arl8b*^{T34N}. Although previous studies reported the generation of Arl8b-deficient mice (Oka et al. 2017; Hashimoto et al. 2019; Saitoh et al. 2019), this was the first attempt to generate KI mice of GTP-binding form and GDP-binding form mutant of Arl8b.

Although it is likely that Arl8b-mediated lysosomal positioning affects function of mTORC1 signaling including cell senescence, nutrient sensing and autophagy (Papadopoli et al. 2019), there was no obvious difference of cell proliferation in neither the *Arl8b*-KO MEF or the *Arl8b*$^{\Delta 9}$ MEF cell line (Figure 4). This result suggests that Arl8b-mediated lysosome positioning does not affect cell proliferation under normal culture condition.

Starvation and recovery treatment changed lysosomal distribution in the WT MEF cells as previous studies using cell lines indicated. As reported by a previous study using the HeLa cells, FBS starvation for 24 h caused juxtanuclear clustering of lysosomes, whereas 30 min recovery treatment by adding amino acids together with serum restored lysosome distribution (Korolchuk et al. 2011). Consistent with the previous study of HeLa cells, I found that FBS starvation for 24 h increased the proportion of perinuclear lysosomes in the control MEFs (Figure 5B). However, it took at least 3 h for lysosomes to start redistributing to the cell periphery and 6 h for the entire redistribution of lysosomes (Figure 5B). This difference in the duration of lysosomal redistribution after the recovery treatment between HeLa cells and MEFs may reflect the different characteristic of cell types.

Knockout of Arl8b in MEFs did not cause a dramatical change of lysosomal positioning. In HeLa cells, it has been shown that the Arl8b silencing increases the proportion of cells with predominantly perinuclear lysosomes (Khatter et al. 2015; Pu et al. 2015). Therefore, I hypothesized, even under a normal condition, MEFs of *Arl8b*-KO or Arl8b GDP-binding form mutant might show perinuclear lysosomal distribution and MEFs from Arl8b GTP-binding form mutants might show more peripheral distribution than the control MEFs. However, there was no obvious difference in lysosome distribution under the normal condition between the control and all four mutants I generated in this study (Figure 11). Another study of HeLa cell demonstrated the overexpression of SKIP, which is an effector for Arl8 (Arl8a and Arl8b), still drove some lysosomes to the cell periphery in the *Arl8b*-KO cells whereas a treatment of the *Arl8b*-KO cells with siRNA against Arl8a completely abolished the effect of SKIP on lysosomal distribution (Guardia et al. 2016). There is a possibility that juxtanuclear clustering of lysosomes was not observed in *Arl8b* mutant MEFs because Arl8a might compensate the loss of function of Arl8b for lysosome positioning in *Arl8b*-KO MEF cells. Arl8a is also localized at the lysosomes and involved in lysosomal positioning (Khatter et al. 2015), but it is not known whether Arl8a can compensate for the loss-of-function of Arl8b. To find out the relationship between Arl8a and Arl8b, expression of Arl8a in *Arl8b*-KO and control MEFs should be investigated.

Under the nutrient deprived status, control and all four Alr8b mutant MEFs similarly showed more predominantly perinuclear distribution of lysosomes compared to cells under the no treatment condition (Figure 10 and 14). There was no difference among genotypes in the ratio at FBS starvation, suggesting that the response to a nutritional insufficient status seems similar among genotypes. Many previous studies indicated Arl8b is involved in lysosomal movement to the cell periphery rather than to the perinuclear region (Bagshaw et

al. 2006; Hofmann and Munro. 2006; Pu et al. 2016) and nutritional insufficient status promotes autophagy (Korolchuk et al. 2011). Autophagosome was known to be formed in the periphery of cells and move centripetally for fusing to juxtanuclear lysosomes (Kimura et al. 2008; Korolchuk et al. 2011). A recent study has shown that lysosomes, which are located a perinuclear region, were more acidic and had higher acid hydrolase activity than lysosomes locating a peripheral region (Johnson et al. 2016). Thus, there is a possibility that an autophagic activity might be different among genotypes. To examine this possibility, the autophagic activity and the expression of autophagy-related genes should be investigated in the Arl8b mutant cells.

A recovery response after starvation was significantly delayed in the *Arl8b*$^{\Delta 9/\Delta 9}$ and *Arl8b*$^{T34N/T34N}$ MEFs compared to the control. Comparison of the average ratios demonstrated both the *Arl8b*$^{\Delta 9/\Delta 9}$ and *Arl8b*$^{T34N/T34N}$ MEFs showed a significantly lower value of the ratio compared to the control MEFs after the recovery treatment for 1 h (Figure 10). Even after 3 h recovery treatment, the *Arl8b*$^{\Delta 9/\Delta 9}$ and *Arl8b*$^{T34N/T34N}$ MEFs did not increase the ratio value (Figure 10). Similar results were obtained when I categorized cells into two groups: cell with dominantly perinuclear lysosomes and cells with dominantly peripheral lysosomes (Figure 14). These results suggest that the Arl8b mutation or Arl8b in its GDP-bound form delays the nutritional response of lysosomes. Additionally, for 6 h recovery treatment, *Arl8b*$^{T34N/T34N}$ MEFs remained to have more perinuclear lysosomes than the control (Figure 10 and 14). On the other hand, a greater number of the *Arl8b*$^{Q75L/Q75L}$ cells showed predominantly peripheral lysosomal pattern than *Arl8b*$^{T34N/T34N}$ MEFs (Figure 14). These results suggest the importance of Arl8b in its GTP-bound form for the redistribution of lysosomes after nutritional recovery. A previous study of NRK cells indicated that cells expressing Arl8b-Q75L increased a speed of lysosome movements compared to expressing normal Arl8b (Hofmann and Munro. 2006).

My finding in this study demonstrates that Arl8b is required for the change of lysosome positioning in response to a replenishment of nutrient availability after starvation.

In addition, the results of *Arl8b*$^{\Delta 9/\Delta 9}$ under the starvation and recovery treatment suggest that the three amino acids which are deleted in the *Arl8b*$^{\Delta 9/\Delta 9}$ cells seem to be important for Arl8b function. Interestingly, the *Arl8b*$^{\Delta 9/\Delta 9}$ cell showed severer phenotype than the *Arl8b*-KO cell. Arl8b contains highly conserved GTP-binding domains (G1-G5), an N-acetylated amphipathic helix and a putative effector domain (Okai et al. 2004; Hofmann and Munro. 2006). The sequence of three amino acids deleted in the Arl8b$^{\Delta 9}$ protein is located between G1 and G2 and neither within the GTP-binding domain nor within the effector domain (Figure 3B). There are two possibilities how the deletion of three amino acids affects the Arl8b protein function. One is that the deletion of three amino acids might cause a structural change of Arl8b protein, and the Arl8b$^{\Delta 9}$ protein may lose a proper Arl8b function and behaves similarly to the Arl8b GDP-binding form mutant. Second is that Arl8b$^{\Delta 9}$ protein may lose its ability to interact its partners. Previous studies indicated that there are two proteins which interact with Arl8b for lysosomal trafficking: kinesin-3 and SKIP. It has been demonstrated that Arl8b and BORC complex regulate the kinesin-1 (KIF5B) and the kinesin-3 (KIF1Bb and KIF1A) proteins for lysosomal peripheral trafficking along different microtubule tracks (Guardia et al. 2016). Arl8b interacts through an intrinsic CC3 domain in kinesin-3, and kinesin-3 preferentially moves lysosomes on perinuclear tracks enriched in acetylated a-tubulin (Guardia et al. 2016; Wu et al. 2013). Second, Arl8b interacts with RUN domain of SKIP and drives lysosome movements to the cell periphery (Guardia et al. 2016; Rosa-Ferreira and Munro. 2011). To examine GTPase activity and interacting effectors of Arl8b$^{\Delta 9}$ protein, affinity assay of Arl8b$^{\Delta 9}$ protein toward GTP and effector proteins is required in the future.

The present findings of this chapter indicate that Arl8b function is essential for lysosomal positioning in response to nutritional recovery after starvation in primary cells. Also, the sequence of three amino acids near the G2 domain is required for Arl8b function.

CHAPTER 2

Behavioral analyses of *Arl8b* gene-edited mice

2.1 INTRODUCTION

In mouse, a previous study revealed that *Arl8b* gene is one of candidate genes for positively regulating the general behavioral activity, which is defined as a locomotor activity in the habituated situation (Kato et al. 2014). Home-cage activity test, which records animal's voluntary movements without any stimuli, is one of the principal ways of measuring the general locomotor activity (Kas et al., 2009; Koide et al. 2000). Previously, it was shown that a wild-derived mouse strain MSM/MS (MSM) showed higher locomotor activity than a laboratory strain C57BL/6J (B6) in the home-cage activity test (Koide et al. 2000). For genetic mapping of the general locomotor activity, consomic strains, which are also known as chromosome substitution strains, were previously generated by replacing any one chromosome of B6 with the corresponding chromosome of MSM (Takada et al. 2008). The home-cage activity test was performed in the established consomic strains and it was previously found that 10 of 18 consomic strains, for chromosome 2T (telomere side), 3,4,6C, (centromere side), 7T, 9, 11, 13, 14 and 15, showed different behavioral activity from B6 (Nishi et al. 2010). This result suggested that multigenic factors located on different chromosomes also regulate the general locomotor activity.

High-resolution genetic mapping of home-cage activity has been subsequently performed by using a series of congenic strains, which carry a small region of chromosome 6 derived from MSM in otherwise B6 genetic background. This study revealed that there were

four loci of chromosome 6 that are associated with the general locomotor activity. In more detail, three loci negatively regulate and one locus positively regulates the general locomotor activity (Kato et al. 2014). *Arl8b* gene was founded in the locus which is important for increasing the general locomotor activity. However, it remains unclear whether *Arl8b* gene affects the general locomotor activity.

Although previous *in vitro* studies indicated that Arl8b is crucial for lysosomal function including lysosomal positioning and autophagy, little is known about the roles of Arl8b *in vivo*. In *C. elegans*, a loss of Arl8 led to an increase in the number of late endosomal-lysosomal compartments, which are smaller in size than those of wild-type (Nakae et al. 2010). In addition, the loss of Arl8 in *C. elegans* resulted in embryonic lethality and this embryonic lethality was rescued by introduction of wild-type Arl8 or GTP-binding form mutant (Arl8b-Q75L) (Nakae et al. 2010). These results have shown that Arl8b is required for normal embryonic development. In mouse, it has been demonstrated that Arl8b is required for the lysosomal degradation of maternal proteins in the visceral yolk sac endoderm (VYSE) which plays an important role in the nutritional supply from mothers to embryos (Oka et al. 2017). Also, Arl8b is involved in the mouse brain development, especially in the neural fold development (Hashimoto et al. 2019). A recent study of mouse models of systemic lupus erythematosus (SLE) indicated that Arl8b can be a new target for therapeutic intervention in SLE (Saitoh et al. 2019). Although the importance of Arl8b in mouse embryogenesis and disease pathogenesis started to be revealed, phenotypic effects of Arl8b still remains unclear.

In this chapter, I examined behavioral phenotype of Arl8b mutants, especially the general locomotor activity. First, I conducted sequence analyses of *Arl8b* genes between B6 and MSM. Also, I compared the expression level of *Arl8b* in several brain regions between MSM and B6 by qRT-PCR. Next, I examined general phenotypes of four kinds of *Arl8b* gene-edited

mutants described in chapter 1: *Arl8b*-KO, $Arl8b^{\Delta 9}$, GTP-bound form mutant $Arl8b^{Q75L}$ and GDP-bound form mutant $Arl8b^{T34N}$. A previous study of *C. elegans* showed that loss of function of Arl8 inhibits viable embryo production by hermaphrodites (Nakae et al. 2010). To check viability of Arl8b mutants, I examined the genotype of progeny made from a crossing heterozygous mice of each mutant. I also compared body weight among genotypes of four mouse strains. I found that homozygous mice for *Arl8b*-KO, $Arl8b^{\Delta 9}$ and $Arl8b^{T34N}$ died around birth whereas homozygous mice for $Arl8b^{Q75L}$ can survive until adulthood. Thus, I performed behavioral tests by using heterozygous mice for *Arl8b*-KO, $Arl8b^{\Delta 9}$, $Arl8b^{T34N}$ and $Arl8b^{Q75L}$, and homozygous mice for $Arl8b^{Q75L}$. For studying the function of Arl8b on the general locomotor activity, four kinds of behavioral tests were conducted: the home-cage activity test, the open-field test, the light and dark box test and the elevated plus maze test. The home-cage activity test was chosen for evaluating the general locomotor activity in a familiar environment. In the open-field test, I investigated the general locomotor activity by measuring mice's ambulation during the test, and emotionality by measuring the time spent in a center area of the apparatus and observing several behavioral components. In the light and dark box test and the elevated plus maze test, which are commonly used to examine anxiety-related behavior, were used to evaluate the emotionality in other situations.

2.1 MATERIALS AND METHODS

Animals

C57BL/6JJcl (B6) mice were purchased from CLEA Japan (Tokyo, Japan). MSM/Ms (MSM) mice were established at NIG. The 10-15 weeks-old male mice were used for quantitative real time PCR (qRT-PCR) and behavioral tests.

RNA isolation, reverse transcription, and quantitative real-time PCR

3-8 males in each strain were used to quantify mRNA levels. The animals were sacrificed by cervical dislocation and decapitation. Brain parts were quickly dissected and kept at -80℃. All tissues were homogenized in Trizol reagent (15596-026, Life Technologies), and the total RNAs were isolated from the homogenates according to manufacturer's protocol followed by DNA digestions with TURBO DNA-free DNase (AM1907, Life Technologies, Japan). First-strand cDNA was synthesized with PrimeScript II 1st strand cDNA Synthesis Kit (6210A, Takara) in the manner determined by manufacturer's instructions. qRT-PCR was carried out with SYBR Premix Ex Taq II (Ti RNaseH Plus) (RB820S, Takara) on a Thermal Cycler Dice Real Time System II (TP900, Takara). The mRNA levels of *Arl8b* gene were normalized to β-actin mRNA levels. Primers for *Arl8b* and β-actin were used in Table 1. The primers for qRT-PCR were designed in the common sequence to MSM and B6. Product size of PCR is same between MSM and B6.

Behavioral Testing

Home-cage activity test

Before the test, mice were kept individually for more than 1 day in their home cage to habituate them to isolation. The home-cage test constituted the recording of individual spontaneous home-cage activity from 6 a.m. on the day after transfer for 3 days. Dark period is from 6 p.m. to 6 a.m. To evaluate the spontaneous behavioral activity of each mouse in their home cage, an infrared sensor (ACTIVITY SENSOR, Ohara Co. Ltd., Tokyo, Japan) was used. This sensor was located above the lid (made from stainless-steel wire) of each cage. The sensor records the motion of the mouse inside the home cage as counts by the sensor. Using this apparatus, many kinds of locomotor activity, such as horizontal locomotion, climbing the cage lid, hanging on the lid, and jumping, could be detected efficiently. In each test session, the test apparatus simultaneously recorded the activity of up to 10 mice in the home cage. The locomotor activity of each 1-min bin was measured for 72 h. The total locomotor activity was quantified using the following two measurements: active time and average locomotor activity (Umemori et al. 2009). Active time was calculated as the total number of minutes in which at least one movement was counted within a 1-min interval. Therefore, the active time estimated the approximate duration of movement. Average locomotor activity, which was an index of ‘‘intensity,’’ was calculated using the formula: average locomotor activity = total locomotor activity / active time. The average locomotor activity reflected the average amount of locomotion over 1 min of active time. For the analyses of temporal patterns, average locomotor activity counts for each 1 h bin over the 3 days were calculated and used as scores for each hour.

Open-field test

The open-field consisted of a square arena (60 x 60 cm) made of white polyvinylchloride plastic board with 40 cm high walls. The arena was lit by incandescent lighting placed 90 cm above the arena. The light level was 365 lux at the center of the arena. The open-field was surrounded by a black curtain except for one side from where the experimenter directly observed the animal's behavior.

For analyzing ambulation, the arena was continuously recorded by a video camera placed over its center and relayed to a video tracking system (Image OF, O'hara & Co. Ltd., Tokyo, Japan). At least 1 hour before the beginning of the test, animals were brought into the test room to minimize the effect of transfer. Each mouse was gently picked up by its tail with tweezers and placed in the same corner of the open-field. During the ten-minute trial, their behavior was observed directly and recorded. The behaviors were recorded including the following 7 behavioral items.

Locomotion: walking and running around the arena.

Leaning-against-wall (Leaning): standing on the hindlimbs with the forelimbs against the wall.

Rearing: standing on the hindlimbs without touching the wall.

Grooming: licking and/or scratching its fur, licking its genitalia and tail.

Face-washing: scrubbing its face with the forelimbs, not followed by grooming

Jumping: jumping vertically.

Pausing: a brief moment of inactivity

At the end of the sessions, the number of defecations and presence of urination were recorded, after which the arena was cleaned with a damp cloth. All the tests were carried out during the light period (13:00-18:00).

Light and Dark box test

After more than one day interval from the home-cage activity test, I performed the light and dark box test using SCANET MV-10LD apparatus (Melquest Co. Ltd. Toyama, Japan). The innate fear behavior to a brightly illuminated environment was measured using the light and dark box test. The apparatus consisted of two compartments, the black and the transparent acrylic chambers (29 x 14 x 15 cm; width x depth x height), separated by a black acrylic board with an entrance of 4cm in diameter between the two chambers. When I started the test, mice were placed individually into the dark chamber. The number of transitions between a light and a dark box, exploratory behaviors (leaning and rearing) and the time spent in the light and the dark box were measured.

Elevated plus maze test

The apparatus used in this study consists of two open arms with low edge (30 x 5 x 0.25 cm; width x depth x height) and two closed arms enclosed by clear acrylic plastic walls (30 x 5 x 15 cm) that extended from a central platform (5 x 5 cm), which was elevated 60 cm above the floor. The apparatus was dimly lit (150 lux). Two opposite arms have high walls to prevent animals from falling off; the other two do not have walls and animals are able to look around/down. Mice were placed individually in the central platform and allowed to move freely for 10 min. Ambulatory activity (cm), the number of entries into the open-arm or closed-arm, and the duration in the open-arm or closed-arm were measured by a video tracking system

(Image EPM; O'hara & Co. ltd., Tokyo, Japan). All tests were carried out during the light period (13:00-18:00).

Statistical analysis

ANOVA was performed to detect the differences between mutant mice and their littermates. Differences were considered to be significant at $p < 0.05$. The calculations were performed using StatView 5.0 (SAS Institute Inc., USA)

2.2 RESULTS

A wild derived strain MSM showed a higher expression of *Arl8b* gene than a laboratory strain B6

Since MSM showed higher locomotor activity than B6 in the home-cage activity test (Koide et al. 2000), there is a possibility that this behavioral difference between MSM and B6 could be caused by a different expression of *Arl8b* gene. First, I conducted a sequence analyses of *Arl8b* genes and found no non-synonymous polymorphisms between MSM and B6. Next, I compared the expression of *Arl8b* gene between MSM and B6 using qRT-PCR. I isolated 5 brain parts from both MSM and B6: cerebellum, midbrain, hippocampus, striatum and cortex. *Arl8b* mRNA expression was detected in all brain tissues that I examined. MSM showed significantly higher expression of *Arl8b* mRNA in the cerebellum (one-way ANOVA, $F(1,12) = 6.070$, $p = 0.0298$) and striatum (one-way ANOVA, $F(1,4) = 8.438$, $p = 0.0439$). Although there is a tendency that *Arl8b* mRNA was expressed at higher levels in midbrain, hippocampus or cortex of MSM than in that of B6, the difference was not statistically significant (Figure 15). It suggests that mice which shows higher locomotor activity like MSM may have higher expression of *Arl8b*.

GTP-binding form of Arl8b is required for perinatal survival

To check the viability of homozygous mice for Arl8b mutants, I performed genotype analysis of progeny from crossing heterozygous mice of each *Arl8b* gene-edited mutant

(Figure 16 and Table 2). The number of embryos at E15.5 and E18.5 and pups at 3-4 weeks old were genotyped. At E15.5, around 20% of the total embryos were homozygote for *Arl8b* mutants in all strains (Figure 16 and Table 2). Similarly, homozygote for all *Arl8b* mutants were detected at E18.5 and the survival of homozygote for Arl8b mutants approached 20% (Figure 16 and Table 2). However, $Arl8^{-/-}$, $Arl8b^{\Delta 9/\Delta 9}$ and $Arl8b^{T34N/T34N}$ embryos were not detected at the age of 3-4 weeks old (Figure 16A, B and D). $Arl8^{-/-}$, $Arl8b^{\Delta 9/\Delta 9}$ and $Arl8b^{T34N/T34N}$ were not detected among the live neonates at one day after birth, but they were detected among the dead neonates at one day after birth (data not shown). Only $Arl8b^{Q75L/Q75L}$ pups were still alive at 3-4 weeks old, but the survival rate of $Arl8b^{Q75L/Q75L}$ pups was only 12.1%, which was lower than the expectation of Mendel's law (Figure 16C and Table 2C). These results suggest that Arl8b GTP-binding form is necessary for perinatal survival.

Homozygotes for *Arl8b* gene-edited mutants showed significantly smaller body weight than their WT littermates

Next, I compared body weight among genotypes. Figure 17 shows the difference in body weight among strains. All of homozygous mice of *Arl8b*-KO, $Arl8b^{\Delta 9}$, $Arl8b^{Q75L}$ and $Arl8b^{T34N}$ were significantly smaller than their WT and heterozygous littermates. Bonferroni / Dunnett test showed a significant difference between $Arl8b^{+/+}$ and $Arl8^{-/-}$ mice ($p < 0.0001$) and between $Arl8^{+/-}$ and $Arl8^{-/-}$ mice ($p < 0.0001$) (Figure 17A). The average scores of the body weight of $Arl8b^{\Delta 9/\Delta 9}$ embryos was statistically smaller than that of both their WT ($p < 0.0001$, Bonferroni / Dunnett test) and $Arl8b^{+/\Delta 9}$ littermates ($p < 0.0001$, Bonferroni / Dunnett test) (Figure 17B). Also, the body weight of $Arl8b^{Q75L/Q75L}$ embryos was markedly smaller in

comparison to their WT and heterozygous littermates (*Arl8b*$^{+/+}$ versus *Arl8b*$^{Q75L/Q75L}$ p = 0.0076, *Arl8b*$^{+/Q75L}$ versus *Arl8b*$^{Q75L/Q75L}$ p = 0.0104, Bonferroni / Dunnett test) (Figure 17C). At an adult stage, only homozygous mice of *Arl8b*^{Q75L} were alive, although the body weight of *Arl8b*$^{Q75L/Q75L}$ mice was smaller than that of their WT littermates or *Arl8b*$^{+/Q75L}$ littermates. Similarly, there was a significant difference in body weight between three genotypes in *Arl8b*^{T34N} (*Arl8b*$^{+/+}$ versus *Arl8b*$^{T34N/T34N}$ p = 0.0004, *Arl8b*$^{+/T34N}$ versus *Arl8b*$^{T34N/T34N}$ p = 0.0017, Bonferroni / Dunnett test) (Figure 17D). These results suggest that the Arl8b dysfunction causes the abnormality of body weight in the embryos.

Arl8b$^{+/\Delta 9}$ mice showed significantly higher locomotor activity than their wild-type littermates

From the results of *Arl8b* expression analysis, *Arl8b* gene is possibly involved in regulating the general locomotor activity. Therefore, I next conducted behavioral analyses of *Alr8b* gene-edited mutants. As mentioned above, *Arl8b*$^{-/-}$, *Arl8b*$^{\Delta 9/\Delta 9}$, and *Arl8b*$^{T34N/T34N}$ mice were lethal, therefore I conducted behavior tests in mice heterozygous for *Arl8b*$^{\Delta 9}$, *Arl8b*-KO and *Arl8b*^{T34N}. In case of *Arl8b*^{Q75L} mice, I performed behavioral analyses of all genotypes.

Arl8b$^{+/\Delta 9}$ *and Arl8b*$^{+/T34N}$ *mice have a tendency to show higher locomotor activity in the home-cage activity test*

In the home-cage activity test, I analyzed the total locomotor activity, the active time and the average locomotor activity during the active time (Figure 18), and the temporal pattern of

the home-cage activity (hour-by-hour) (Figure 19). Figure18A indicates the total locomotor activities of four *Arl8b* gene-edited mice; *Arl8b*-KO, $Arl8b^{\Delta 9}$, $Arl8b^{T34N}$ and $Arl8b^{Q75L}$. No significant difference was detected between the $Arl8b^{+/-}$ mice and their WT littermates in all analyses of the home-cage activity test (Figure 18 and 19). The $Arl8b^{+/\Delta 9}$ mice tended to move slightly more than their WT littermates, but it was not significantly different in the total locomotor activity, the active time or the average locomotor activity (Figure 18).

To examine the effect of the GTPase activity of Arl8b protein on the home-cage activity, I also performed behavioral analyses of the Arl8b GTP/GDP-bound form mutant. $Arl8b^{T34N}$ mutants showed relatively higher total locomotor activity and average locomotor activity, but the difference between the $Arl8b^{+/T34N}$ mutants and their WT littermates was not statistically significant (Figure 18). The $Arl8b^{Q75L}$ mice did not show any abnormal behaviors in the home-cage activity test (Figure 18). Interestingly, the $Arl8b^{+/\Delta 9}$ and $Arl8b^{+/T34N}$ mice showed higher locomotor activity during the early phase of the dark period (Figure 19 B and D), whereas the $Arl8b^{+/-}$ and $Arl8b^{Q75L/75L}$ mutants did not differ from their WT littermates (Figure 19 A and C).

$Arl8b^{+/\Delta 9}$ mice traveled longer distance and showed more vertical activity in the open field test

Figure 20 and 21 indicated results of behavioral components in the open-field test. The $Arl8b^{+/-}$ mice showed a similar behavior to their WT littermates (Figure 20 and 21). On the other hand, one-way ANOVA indicated a significant effect of the *Arl8b* gene mutation on three behavioral components; leaning ($F(1, 25) = 6.672$, $p = 0.0160$, one-way ANOVA) (Figure 20A), jumping ($F(1, 25) = 5.875$, $p = 0.0229$, one-way ANOVA) (Figure 20C), and vertical activity ($F(1, 25) = 9.845$, $p < 0.01$, one-way ANOVA) (Figure 20D). Especially the $Arl8b^{+/\Delta 9}$

mice showed leaning behaviors much more often than their WT littermates. 50% of the *Arl8b*$^{+/\Delta 9}$ mice (7 of 14 mice) showed jumping behaviors while none of their WT (0 of 13 mice) littermates showed jumping. Pausing and face washing behavior that are categorized as anxiety behaviors were not significantly different (Figure 21A and B). Among the *Arl8b*^{Q75L} strains, there was no obvious difference in any behavioral components (Figure 20 and 21). The *Arl8b*$^{+/T34N}$ mice showed a tendency to have a greater number of leaning behaviors than their WT littermates while a significant difference was not detected (Figure 20A).

Figure 22A shows the average traveled distance and Figure 22B indicates the temporal traveled distance during the 10 minutes of the open-field test. Although the *Arl8b*$^{+/-}$ and *Arl8b*$^{Q75L/Q75L}$ mice did not show any difference from their littermates (Figure 22A), the *Arl8b*$^{+/\Delta 9}$ mice markedly traveled longer than their WT littermates ($F(1, 26) = 24.132$, $p < 0.001$, one-way ANOVA) (Figure 22A). The *Arl8b*$^{+/T34N}$ mice tended to travel the longer distance (Figure 22A and B). The time spent in the center area of the open-field was not statistically significant between the *Arl8b*$^{+/-}$ mice and their WT littermates, between the *Arl8b*$^{+/\Delta 9}$ mice and their WT littermates, between the *Arl8b*$^{Q75L/Q75L}$ mice and their WT littermates, or between the *Arl8b*$^{+/T34N}$ mice and their WT littermates (Figure 22C).

Arl8b$^{+/\Delta 9}$ *mice showed significantly higher locomotor activity in the light and dark box test but not in the elevated plus maze test*

Figure 23 shows the results of the light and dark box test. The *Arl8b*$^{+/-}$ mice did not show any defects in this test. On the other hand, the *Arl8b*$^{+/\Delta 9}$ mice showed higher activity in the dark box ($F(1, 25) = 4.741$, $p = 0.0391$, one-way ANOVA) (Figure 23D). While there was no

statistical difference between the *Arl8b*$^{+/\Delta 9}$ mice and their WT littermates in the number of transition activity and vertical activity in the dark box, there was a trend of *Arl8b*$^{+/\Delta 9}$ mice increasing these compared to their WT littermates (Figure 23F and H). In the elevated plus maze test, no significant difference was detected either between the *Arl8b*$^{+/-}$ mice and their WT littermates, or between the *Arl8b*$^{+/\Delta 9}$ mice and their WT littermates (Figure 24).

No difference in Arl8b expression level between Arl8b$^{+/\Delta 9}$ *mice and their WT littermates*

The behavioral results suggested that *Arl8b*$^{+/\Delta 9}$ mice increased the general locomotor activity. Therefore, I checked the expression level of *Arl8b* in the cerebellum, midbrain and cortex of *Arl8b*$^{+/\Delta 9}$ and their WT littermates as shown in Figure 25. There was no significant difference in the expression level of Arl8b between *Arl8b*$^{+/\Delta 9}$ and their WT littermates.

2.3 DISCUSSION

Expression analysis of *Arl8b* revealed that MSM mice showed higher expression of Arl8b mRNA in the cerebellum and striatum than B6. Since MSM mice has higher locomotor activity than B6 in the home-cage activity test (Nishi et al. 2010), my results originally seemed to indicate a possible relationship between the higher activity in the home-cage and the increased *Arl8b* expression.

Genotype analysis of progeny obtained from crossing heterozygous mice of each *Arl8b* gene-edited mutants was consistent with the previous study of *C.elegans* (Nakae et al. 2010). In *C. elegans*, a loss of Arl8 inhibits viable embryo production from hermaphrodites (Nakae et al. 2010). This embryonic lethality in Arl8b deficient animals was rescued by introducing wild-type Arl8 or GTP-binding form Arl8-Q75L in *C. elegans* (Nakae et al. 2010). Similarly, no pups of $Arl8^{-/-}$ or GDP-binding form mutant $Arl8b^{T34N//T34N}$ survived until the age of 3-4 weeks old although GTP-binding form mutant $Arl8b^{Q75L/Q75L}$ were alive (Figure 16 and Table 2). Also, I found $Arl8^{-/-}$, $Arl8b^{\Delta 9/\Delta 9}$ and $Arl8b^{T34N//T34N}$ neonates died after birth within one day. Therefore, my results indicated that Arl8b GTP-binding form may be required for perinatal survival. For normal embryogenesis, embryos need a large amount of amino acid to support massive cell proliferation. To supply nutrients to embryos from maternal proteins, endocytosis has an important role. It has been demonstrated that VYSE exhibited defective endocytic trafficking to the lysosome in the $Arl8b^{-/-}$ embryos (Oka et al 2017). Impaired endocytic trafficking to lysosomes induced an accumulation of endocytosed maternal proteins in VYSE, resulting in a reduction of amino acid levels and smaller body size in the $Arl8b^{-/-}$ embryos (Oka et al 2017). From these previous studies and my own results of MEF cells in chapter 1, I hypothesized that homozygote for *Arl8b*-KO, $Arl8b^{\Delta 9}$ and $Arl8b^{T34N}$ embryos might show abnormal body

weight but *Arl8b*^{Q75L} might be similar to wild-type. However, all homozygous mice of the Arl8b mutants including the *Arl8b*$^{Q75L/Q75L}$ mice showed much smaller body weight than their WT littermates. In addition, adult mouse of *Arl8b*^{Q75LQ75L} showed smaller body size and body weight compared to their heterozygous and WT littermates. It suggests that keeping GTP-binding form may not be sufficient and the exchange between GTP and GDP may be necessary for proper body size growth.

Amino acid deficiency may explain the lethality of homozygotes for *Arl8b*-KO, *Arl8b*$^{\Delta 9}$ and *Arl8b*^{T34N}. At early neonatal stages, autophagy plays an essential role in maintaining amino acid levels. Soon after birth, nutrient supply from mother is suddenly interrupted, and neonates encounter severe starvation until supply can be restored through milk nutrients (Medina et al. 1996). During this neonatal starvation period, amino acid supply through autophagic degradation of 'self' proteins is important for the maintenance of amino acid levels (Kuma et al. 2004; Komatsu et al. 2005; Sou et al. 2008). A previous study showed that *Arl8b*-KO embryos had a lower level of amino acids and died after birth (Oka et al 2017). In chapter 1, I revealed that the Arl8b mutation affects lysosomal positioning during recovery after starvation. Therefore, there is a possibility is that cells might not be able to quickly respond to nutrient supply through milk in *Arl8b*-KO, *Arl8b*$^{\Delta 9}$ and *Arl8b*^{T34N} embryos. To examine this possibility, the level of amino acids should be investigated in the future.

Amino acid deficiency may lead to the neonatal impairment. Atg5-deficient mice exhibit a severe reduction in the total amount of amino acid and die at around 12 h after birth, but lifespan of Atg5-deficient mice can be prolonged by forced milk feeding (Kuma et al. 2004). Atg5 belongs to Atg12 conjunction system, which is essential for the formation of preautophagosomes (Mizushima et al. 2001). Also, it has been indicated that Atg5-null mice showed neonatal lethality because of neuronal dysfunction caused by the autophagy

impairment, resulting in suckling failure (Yoshii et al. 2016). Therefore, the neonatal dysfunction of autophagy in the neuronal system may induce suckling failure. The previous study showed that Arl8b is essential for the brain development (Oka et al. 2017). Histological analysis and expression analysis of autophagy-related genes in *Arl8b* mutants are required.

It should be noted that homozygous mice of *Arl8b*$^{\Delta 9}$ and *Arl8b*^{T34N} seemed to have a difficulty in breathing. When I performed a cesarean section of these embryos at E19.5 or E18.5 and observed whether they can breathe properly, they appeared to have a difficulty in breathing and died within 30 min while their WT littermates were alive. Double KO mice of UNC51-like kinase 1 (ULK1) and ULK2, which are precursors of the autophagosome (Itakura and Mizushima. 2010), died because of impairment of lung function (Cheong et al. 2014). ULK1 is phosphorylated by mTORC1 activity in nutrient sufficient status, whereas mTORC1 inactivation induces dephosphorylation of ULK1, resulting in promoting the formation of the phagophore. My results of MEFs are also consistent with the relationship between mTORC1 activity and Arl8b activity during recovery after starvation. Therefore, it is possible that *Arl8b* mutant embryos might have impaired the respiration system. To examine this possibility, gross and histological characterization of heart and lung in *Arl8b* gene mutants should be investigated.

My behavioral analyses of *Arl8b* gene-edited mutants indicated that Arl8b affects the general locomotor behavior in mice. A previous behavioral study in the truncated mutant mice of BORC subunit BORCS7, which plays a role in the recruitment of Arl8 toward lysosomes, showed severe deficits in motor tasks dependent on hind limb function (Snouwaert et al. 2018). As Arl8b was previously found as a candidate gene which may increase the general locomotor activity (Kato et al. 2014) and my result showed that the expression level of Arl8b is higher in the strain which showed higher general locomotor activity, I hypothesized that

Arl8b knock out might result in a decrease of the general locomotor activity. However, in the home-cage activity test, *Arl8b*$^{+/\Delta 9}$ and *Arl8b*$^{+/T34N}$ mice had a tendency to have higher locomotor activity in the early phase of the dark period in the home-cage (Figure 19). Also, *Arl8b*$^{+/\Delta 9}$ showed significantly higher locomotor activity in the open-field test and the light and dark box test. Similar tendency was observed in *Arl8b*$^{+/T34N}$ mice. On the other hand, *Arl8b*$^{+/-}$ mice did not show any behavioral abnormality (Figure 22 and 23). There are three non-mutually exclusive possible reasons why phenotypic change was detected in *Arl8b*$^{+/\Delta 9}$ but not in either *Arl8b*$^{+/-}$ or *Arl8b*$^{+/T34N}$ mutant. As I performed behavioral tests in heterozygote for *Arl8b*-KO and *Arl8b*^{T34N} mutants, the wild-type allele of Arl8b exists in the heterozygous mice and that may rescue the behavioral phenotype. Behavioral tests of conditional homozygous knockout mice of Arl8b at an adult stage can answer whether the WT allele of Arl8b can compensate the behavioral phenotype. Second, the function of Arl8b might be compensated by its paralog Arl8a. Expression analysis of the *Arl8a* gene in *Arl8b*-KO and *Arl8b*^{T34N} mutants might be helpful to examine this possibility. Third, Arl8b$^{\Delta 9}$ protein may function dominantly than the normal Arl8b protein. As the Arl8b$^{\Delta 9/\Delta 9}$ MEFs showed severer defect in lysosomal positioning than *Arl8b*-KO in chapter 1, it is possible that Arl8b$^{\Delta 9}$ allele may be dominant over the normal allele.

Arl8b$^{+/\Delta 9}$ showed higher locomotor activity in several behavioral tests, but this phenotype was dissimilar to MSM. Previously it has been revealed that MSM showed significantly longer active time and average activity in the home-cage activity test whereas MSM showed shorter ambulation than B6 in the open field test (Nishi et al. 2010; Takahashi et al. 2006). On the other hand, *Arl8b*$^{+/\Delta 9}$ mice had a tendency to have the longer active time in the home-cage activity test, but the longer ambulation time in the open field test. Also, MSM showed a higher expression of *Arl8b* gene than B6 while *Arl8b*$^{+/\Delta 9}$ did not show any difference in expression

levels from their WT littermates. Other genes near *Arl8b* may be causing the behavioral differences between B6 and MSM. The locus, which was found important for increasing the general locomotor activity, also contains two other genes: *Bhlhe40*, *Edem1* (Kato et al. 2014). Bhlhe40 is a member of the basic helix-loop-helix family and a key regulator of both inflammation and pathogen control (Cook et al., 2020). EdemI is a type II endoplasmic reticulum transmembrane protein that affects trimming of mannose residues, which is required for the targeting of misfolded glycoproteins to endoplasmic reticulum-associated degradation in mammalian cells (Hosokawa et al., 2001; Olivari et al., 2006). As *Edem1* has already been shown to be unrelated to the general locomotor activity (unpublished data, Koide lab), *Bhlhe40* gene may be a good candidate gene.

The striatum has important roles in controlling voluntary movement, learning and motivational processes, while the cerebellum is involved in maintaining the balance and the coordination of voluntary movements. A previous study of the wheel running test, which is another test for measuring the general locomotor activity, revealed that the wheel running promotes neuroplasticity in the striatum and this plasticity contributed to stress-resistance (Marais et al. 2009). Also, it has been revealed that striatal dopamine release is negatively correlated with an average distance of the voluntary wheel running (Tarr et al. 2004). Furthermore, another study of wheel running reported that the expression of dopamine-receptor 1 in striatum was decreased in congenic strains which show higher locomotor activity than in congenic strains that show lower activity (Yang et al. 2012). In general, the running wheel activity is considered as a model of a voluntary exercise (Kelly and Pomp 2013; Rezende et al. 2009) while the general locomotor activity in the home-cage is considered as a model of spontaneous physical activity (Garland et al. 2011). It was previously indicated that mouse with an access to a running wheel showed higher activity in the home-cage

(deVisser et al. 2005), suggesting that running wheel activity and home-cage activity are not independent. In addition, a previous report of LMTK3 KO mice indicated LMTK-KO mice showed that locomotor abnormality and LMTK is involved in the endocytic trafficking of N-methyl-D-aspartate receptors, a type of ionotropic glutamate receptor (Inoue et al. 2014). Arl8b may possibly be involved in the dopaminergic signaling in the striatum. Future analysis on a neurochemical difference in monoamines and their metabolite levels in the striatum between *Arl8b*$^{+/\Delta 9}$ and WT mice may help to test the possibility.

CONCLUSION

This study demonstrated the role of Alr8b GTPase activity at cellular and behavioral levels by using *Arl8b* gene-edited mutant mice. Arl8b GDP-form mutation (Arl8b-T34N) induced significant delay of lysosomal redistribution after nutritional replenishment in MEF cells whereas Arl8b GTP-form mutation (Arl8b-Q75L) did not. This result indicates that Arl8b function is essential for quick response to nutritional recovery after starvation through lysosomal positioning. Also, the sequence of three amino acids, which is deleted in $Arl8b^{\Delta 9}$, may be important for an appropriate Arl8b function, because it showed a similar phenotype to Arl8b-T34N. Interestingly, $Arl8b^{+/\Delta 9}$ and $Arl8b^{+/T34N}$ mice showed a behavioral change in the locomotor activity compared to the wild-type mice, whereas $Arl8b^{Q75L/Q75L}$ mice did not show any difference from their wild-type littermate. This result suggests that the Arl8b mutation affects behaviors. Taking both of the cellular and the behavioral analyses into consideration, there is a possibility that Arl8b dysfunction for lysosomal positioning might affect behaviors. Also, my results suggest that the sequence of three amino acids deleted in $Arl8b^{\Delta 9}$ mouse, is crucial for the proper functions of Arl8b, although it is not located at neither the GTP-binding domain nor the effector domain. However, it still remains unclear whether Arl8b affects metabolic signaling such as mTORC1 pathway through the lysosomal positioning and how Arl8b-mediated lysosomal positioning affects behaviors in mouse. The relationships among Arl8b function, metabolic signaling, and brain regions which affect behavioral changes in these mutant mice should be investigated.

ACKNOWLEDGMENT

To perform this study and write up this thesis, I had many helps and advices from many people. This work was not able to be done without those supports.

I would like to thank my supervisor, Dr. Tsuyoshi Koide, letting me study freely and support general things to spend my PhD course. I am thankful to Dr. Keiko Takanami for her technical support and advice. I am grateful to Dr. Akira Tanave, who always helped me how to do behavioral and genetic analyses, and gave me helpful suggestions. I thank Mr. Yuji Imai and Ms. Motoko Nihei for helping me to make genome editing mice by CRISPR/Cas 9gene editing technique. I would like to express my gratitude to Ms. Akiko Murofushi for supporting my student affairs and daily life. I appreciate to Ms. Kumiko Takahashi and Mr. Kyohei Kurosawa for their kindly care of the mice. I am thankful to all members of Mammalian Genomics Laboratory and animal facility at NIG for generous kindness.

I am very grateful to my committee members: Dr. Jun Kitano, Dr. Tatsumi Hirata, Dr. Fumi Kubo and Dr. Takuji Iwasato. Whenever I faced a challenge during my study, they helped me and supported in various ways. I am profoundly thankful to Dr. Rieko Ajima who kindly taught me Immunocytochemistry protocol of MEF cells, gave valuable advices related to cell culture. I thank Mr. Makoto Kiso who taught me a basic knowledge of cell culture and isolation of MEF cells. Cell culture work would not have been possible without their help. I would like to express the deepest appreciation to Dr. Asano Ishikawa for helping and supporting me when I encountered obstacles and difficulties during my PhD. I appreciate many NIG people who gave me a lot of suggestions and advices at NIG poster presentation and NIG colloquium.

I also acknowledge Dr. Kontani for providing Arl8 antibody.

This study was supported by the Japan Society for the Promotion of Science.

REFERENCES

Abe, K., Noguchi, H., Tagawa, K., Yuzuriha, M., Toyoda, A., Kojima, T., Ezawa, K., Saitou, N., Hattori, M., Sakaki, Y., Moriwaki, K., & Shiroishi, T. (2004). Contribution of Asian mouse subspecies Mus musculus molossinus to genomic constitution of strain C57BL/6J, as defined by BAC-end sequence-SNP analysis. *Genome research*, *14*(12), 2439–2447.

Alge, C. S., Hauck, S. M., Priglinger, S. G., Kampik, A., & Ueffing, M. (2006). Differential protein profiling of primary versus immortalized human RPE cells identifies expression patterns associated with cytoskeletal remodeling and cell survival. *Journal of proteome research, 5*(4), 862–878.

Bagshaw, R. D., Callahan, J. W., & Mahuran, D. J. (2006). The Arf-family protein, Arl8b, is involved in the spatial distribution of lysosomes. *Biochemical and biophysical research communications*, *344*(4), 1186–1191.

Berger, Z., Ravikumar, B., Menzies, F. M., Oroz, L. G., Underwood, B. R., Pangalos, M. N., Schmitt, I., Wullner, U., Evert, B. O., O'Kane, C. J., & Rubinsztein, D. C. (2006). Rapamycin alleviates toxicity of different aggregate-prone proteins. *Human molecular genetics*, *15*(3), 433–442.

Carroll, B., & Korolchuk, V. I. (2018). Nutrient sensing, growth and senescence. *The FEBS journal*, *285*(11), 1948–1958.

Caron, A., Richard, D., & Laplante, M. (2015). The Roles of mTOR Complexes in Lipid Metabolism. *Annual review of nutrition*, *35*, 321–348.

Chen, B., Gilbert, L. A., Cimini, B. A., Schnitzbauer, J., Zhang, W., Li, G. W., Park, J., Blackburn, E. H., Weissman, J. S., Qi, L. S., & Huang, B. (2013). Dynamic imaging of genomic loci in living human cells by an optimized CRISPR/Cas system. *Cell*, *155*(7), 1479–1491.

Cheong, H., Wu, J., Gonzales, L. K., Guttentag, S. H., Thompson, C. B., & Lindsten, T. (2014). Analysis of a lung defect in autophagy-deficient mouse strains. *Autophagy, 10*(1), 45–56.

Chua, K. F., Mostoslavsky, R., Lombard, D. B., Pang, W. W., Saito, S., Franco, S., Kaushal, D., Cheng, H. L., Fischer, M. R., Stokes, N., Murphy, M. M., Appella, E., & Alt, F. W. (2005). Mammalian SIRT1 limits replicative life span in response to chronic genotoxic stress. *Cell metabolism*, *2*(1), 67–76.

Cook, M. E., Jarjour, N. N., Lin, C. C., & Edelson, B. T. (2020). Transcription Factor Bhlhe40 in Immunity and Autoimmunity. *Trends in immunology*, S1471-4906(20)30209-X.

Dossou, A. S., & Basu, A. (2019). The Emerging Roles of mTORC1 in Macromanaging Autophagy. *Cancers, 11*(10), 1422.

Dozynkiewicz, M. A., Jamieson, N. B., Macpherson, I., Grindlay, J., van den Berghe, P. V., von Thun, A., Morton, J. P., Gourley, C., Timpson, P., Nixon, C., McKay, C. J., Carter, R., Strachan, D., Anderson, K., Sansom, O. J., Caswell, P. T., & Norman, J. C. (2012). Rab25 and CLIC3 collaborate to promote integrin recycling from late endosomes/lysosomes and drive cancer progression. *Developmental cell*, *22*(1), 131–145.

Encarnação, M., Espada, L., Escrevente, C., Mateus, D., Ramalho, J., Michelet, X., Santarino, I., Hsu, V. W., Brenner, M. B., Barral, D. C., & Vieira, O. V. (2016). A Rab3a-dependent complex essential for lysosome positioning and plasma membrane repair. *The Journal of cell biology*, *213*(6), 631–640.

Eriksson, M., Rasmussen, F., & Tynelius, P. (2006). Genetic factors in physical activity and the equal environment assumption-- the Swedish young male twins study. *Behavior genetics*, *36*(2), 238–247.

Fraldi, A., Klein, A. D., Medina, D. L., & Settembre, C. (2016). Brain Disorders Due to Lysosomal Dysfunction. *Annual review of neuroscience*, *39*, 277–295.

Garg, S., Sharma, M., Ung, C., Tuli, A., Barral, D. C., Hava, D. L., Veerapen, N., Besra, G. S., Hacohen, N., & Brenner, M. B. (2011). Lysosomal trafficking, antigen presentation, and microbial killing are controlled by the Arf-like GTPase Arl8b. *Immunity*, *35*(2), 182–193.

Garland, T., Jr, Schutz, H., Chappell, M. A., Keeney, B. K., Meek, T. H., Copes, L. E., Acosta, W., Drenowatz, C., Maciel, R. C., van Dijk, G., Kotz, C. M., & Eisenmann, J. C. (2011). The biological control of voluntary exercise, spontaneous physical activity and daily energy expenditure in relation to obesity: human and rodent perspectives. *The Journal of experimental biology*, *214*(Pt 2), 206–229.

Goto, T., Tanave, A., Moriwaki, K., Shiroishi, T., & Koide, T. (2013). Selection for reluctance to avoid humans during the domestication of mice. *Genes, brain, and behavior*, *12*(8), 760–770.

Guardia, C. M., Farías, G. G., Jia, R., Pu, J., & Bonifacino, J. S. (2016). BORC Functions Upstream of Kinesins 1 and 3 to Coordinate Regional Movement of Lysosomes along Different Microtubule Tracks. *Cell reports*, *17*(8), 1950–1961.

Haeussler, M., Schönig, K., Eckert, H., Eschstruth, A., Mianné, J., Renaud, J. B., Schneider-Maunoury, S., Shkumatava, A., Teboul, L., Kent, J., Joly, J. S., & Concordet, J. P. (2016). Evaluation of off-target and on-target scoring algorithms and integration into the guide RNA selection tool CRISPOR. *Genome biology*, *17*(1), 148.

Hashimoto, K., Yamaguchi, Y., Kishi, Y., Kikko, Y., Takasaki, K., Maeda, Y., Matsumoto, Y., Oka, M., Miura, M., Ohata, S., Katada, T., & Kontani, K. (2019). Loss of the small GTPase Arl8b results in abnormal development of the roof plate in mouse embryos. Genes to cells : d*evoted to molecular & cellular mechanisms*, *24*(6), 436–448.

Helms, H. C., Abbott, N. J., Burek, M., Cecchelli, R., Couraud, P. O., Deli, M. A., Förster, C., Galla, H. J., Romero, I. A., Shusta, E. V., Stebbins, M. J., Vandenhaute, E., Weksler, B., &

Brodin, B. (2016). In vitro models of the blood-brain barrier: An overview of commonly used brain endothelial cell culture models and guidelines for their use. *Journal of cerebral blood flow and metabolism: official journal of the International Society of Cerebral Blood Flow and Metabolism, 36*(5), 862–890.

Hofmann, I., & Munro, S. (2006). An N-terminally acetylated Arf-like GTPase is localised to lysosomes and affects their motility. *Journal of cell science*, *119*(Pt 8), 1494–1503.

Inoue, T., Hoshina, N., Nakazawa, T., Kiyama, Y., Kobayashi, S., Abe, T., Yamamoto, T., Manabe, T., & Yamamoto, T. (2014). LMTK3 deficiency causes pronounced locomotor hyperactivity and impairs endocytic trafficking. *The Journal of neuroscience : the official journal of the Society for Neuroscience*, *34*(17), 5927–5937.

Itakura, E., & Mizushima, N. (2010). Characterization of autophagosome formation site by a hierarchical analysis of mammalian Atg proteins. *Autophagy*, *6*(6), 764–776.

Johnson, D. E., Ostrowski, P., Jaumouillé, V., & Grinstein, S. (2016). The position of lysosomes within the cell determines their luminal pH. *The Journal of cell biology*, *212*(6), 677–692

Jongsma, M. L., Berlin, I., Wijdeven, R. H., Janssen, L., Janssen, G. M., Garstka, M. A., Janssen, H., Mensink, M., van Veelen, P. A., Spaapen, R. M., & Neefjes, J. (2016). An ER-Associated Pathway Defines Endosomal Architecture for Controlled Cargo Transport. *Cell*, *166*(1), 152–166.

Kahn, R. A., Cherfils, J., Elias, M., Lovering, R. C., Munro, S., & Schurmann, A. (2006). Nomenclature for the human Arf family of GTP-binding proteins: ARF, ARL, and SAR proteins. *The Journal of cell biology*, *172*(5), 645–650.

Kas, M. J., de Mooij-van Malsen, J. G., de Krom, M., van Gassen, K. L., van Lith, H. A., Olivier, B., Oppelaar, H., Hendriks, J., de Wit, M., Groot Koerkamp, M. J., Holstege, F. C., van Oost, B. A., & de Graan, P. N. (2009). High-resolution genetic mapping of mammalian motor activity levels in mice. *Genes, brain, and behavior*, *8*(1), 13–22.

Kato, S., Ishii, A., Nishi, A., Kuriki, S., & Koide, T. (2014). Segregation of a QTL cluster for home-cage activity using a new mapping method based on regression analysis of congenic mouse strains. *Heredity*, *113*(5), 416–423.

Kelly, S. A., & Pomp, D. (2013). Genetic determinants of voluntary exercise. *Trends in genetics : TIG*, *29*(6), 348–357.

Khatter, D., Sindhwani, A., & Sharma, M. (2015). Arf-like GTPase Arl8: Moving from the periphery to the center of lysosomal biology. *Cellular logistics, 5*(3), e1086501.

Kimura, S., Noda, T., & Yoshimori, T. (2008). Dynein-dependent movement of autophagosomes mediates efficient encounters with lysosomes. *Cell structure and function*, *33*(1), 109–122.

Koide, T., Moriwaki, K., Ikeda, K., Niki, H., & Shiroishi, T. (2000). Multi-phenotype behavioral characterization of inbred strains derived from wild stocks of Mus musculus. *Mammalian genome : official journal of the International Mammalian Genome Society*, *11*(8), 664–670.

Komatsu, M., Waguri, S., Ueno, T., Iwata, J., Murata, S., Tanida, I., Ezaki, J., Mizushima, N., Ohsumi, Y., Uchiyama, Y., Kominami, E., Tanaka, K., & Chiba, T. (2005). Impairment of starvation-induced and constitutive autophagy in Atg7-deficient mice. *The Journal of cell biology, 169*(3), 425–434.

Korolchuk, V. I., Saiki, S., Lichtenberg, M., Siddiqi, F. H., Roberts, E. A., Imarisio, S., Jahreiss, L., Sarkar, S., Futter, M., Menzies, F. M., O'Kane, C. J., Deretic, V., & Rubinsztein, D. C. (2011). Lysosomal positioning coordinates cellular nutrient responses. *Nature cell biology*, *13*(4), 453–460.

Koyner, J., Demarest, K., McCaughran, J., Jr, Cipp, L., & Hitzemann, R. (2000). Identification and time dependence of quantitative trait loci for basal locomotor activity in the BXD recombinant inbred series and a B6D2 F2 intercross. *Behavior genetics*, *30*(3), 159–170.

Kuma, A., Hatano, M., Matsui, M., Yamamoto, A., Nakaya, H., Yoshimori, T., Ohsumi, Y., Tokuhisa, T., & Mizushima, N. (2004). The role of autophagy during the early neonatal starvation period. *Nature, 432*(7020), 1032–1036.

Lamming, D. W., & Bar-Peled, L. (2019). Lysosome: The metabolic signaling hub. *Traffic (Copenhagen, Denmark)*, *20*(1), 27–38.

Li, Y., Kelly, W. G., Logsdon, J. M., Jr, Schurko, A. M., Harfe, B. D., Hill-Harfe, K. L., & Kahn, R. A. (2004). Functional genomic analysis of the ADP-ribosylation factor family of GTPases: phylogeny among diverse eukaryotes and function in C. elegans. *FASEB journal : official publication of the Federation of American Societies for Experimental Biology*, *18*(15), 1834–1850.

Lowe, S. W., Jacks, T., Housman, D. E., & Ruley, H. E. (1994). Abrogation of oncogene-associated apoptosis allows transformation of p53-deficient cells. *Proceedings of the National Academy of Sciences of the United States of America*, *91*(6), 2026–2030.

Luzio, J. P., Pryor, P. R., & Bright, N. A. (2007). Lysosomes: fusion and function. *Nature reviews. Molecular cell biology*, *8*(8), 622–632.

Marais, L., Stein, D. J., & Daniels, W. M. (2009). Exercise increases BDNF levels in the striatum and decreases depressive-like behavior in chronically stressed rats. *Metabolic brain disease*, *24*(4), 587–597.

Martina, J. A., Chen, Y., Gucek, M., & Puertollano, R. (2012). MTORC1 functions as a transcriptional regulator of autophagy by preventing nuclear transport of TFEB. *Autophagy*, *8*(6), 903–914.

Medina, J. M., Tabernero, A., Tovar, J. A., & Martín-Barrientos, J. (1996). Metabolic fuel utilization and pyruvate oxidation during the postnatal period. *Journal of inherited metabolic disease, 19*(4), 432–442.

Miyake, K., Saitoh, S. I., Sato, R., Shibata, T., Fukui, R., & Murakami, Y. (2019). Endolysosomal compartments as platforms for orchestrating innate immune and metabolic sensors. *Journal of leukocyte biology, 106*(4), 853–862.

Mizushima, N., Yamamoto, A., Hatano, M., Kobayashi, Y., Kabeya, Y., Suzuki, K., Tokuhisa, T., Ohsumi, Y., & Yoshimori, T. (2001). Dissection of autophagosome formation using Apg5-deficient mouse embryonic stem cells. *The Journal of cell biology, 152*(4), 657–668.

Moriwaki, K., Miyashita, N., Mita, A., Gotoh, H., Tsuchiya, K., Kato, H., Mekada, K., Noro, C., Oota, S., Yoshiki, A., Obata, Y., Yonekawa, H., & Shiroishi, T. (2009). Unique inbred strain MSM/Ms established from the Japanese wild mouse. *Experimental animals*, *58*(2), 123–134.

Mukhopadhyay, R. (2016). Lively lysosomes. *ASBMB Today*, *15*, 7.

Nakae, I., Fujino, T., Kobayashi, T., Sasaki, A., Kikko, Y., Fukuyama, M., Gengyo-Ando, K., Mitani, S., Kontani, K., & Katada, T. (2010). The arf-like GTPase Arl8 mediates delivery of endocytosed macromolecules to lysosomes in Caenorhabditis elegans. *Molecular biology of the cell*, *21*(14), 2434–2442.

Nakamura, S., & Yoshimori, T. (2017). New insights into autophagosome-lysosome fusion. *Journal of cell science*, *130*(7), 1209–1216.

Nishi, A., Ishii, A., Takahashi, A., Shiroishi, T., & Koide, T. (2010). QTL analysis of measures of mouse home-cage activity using B6/MSM consomic strains. *Mammalian genome : official journal of the International Mammalian Genome Society*, *21*(9-10), 477–485.

Oka, M., Hashimoto, K., Yamaguchi, Y., Saitoh, S. I., Sugiura, Y., Motoi, Y., Honda, K., Kikko, Y., Ohata, S., Suematsu, M., Miura, M., Miyake, K., Katada, T., & Kontani, K. (2017). Arl8b is required for lysosomal degradation of maternal proteins in the visceral yolk sac endoderm of mouse embryos. *Journal of cell science*, *130*(20), 3568–3577.

Okai, T., Araki, Y., Tada, M., Tateno, T., Kontani, K., & Katada, T. (2004). Novel small GTPase subfamily capable of associating with tubulin is required for chromosome segregation. *Journal of cell science*, *117*(Pt 20), 4705–4715.

Olivari, S., Cali, T., Salo, K. E., Paganetti, P., Ruddock, L. W., & Molinari, M. (2006). EDEM1 regulates ER-associated degradation by accelerating de-mannosylation of folding-defective polypeptides and by inhibiting their covalent aggregation. *Biochemical and biophysical research communications*, *349*(4), 1278–1284.

Pan, C., Kumar, C., Bohl, S., Klingmueller, U., & Mann, M. (2009). Comparative proteomic phenotyping of cell lines and primary cells to assess preservation of cell type-specific functions. *Molecular & cellular proteomics: MCP, 8*(3), 443–450.

Papadopoli, D., Boulay, K., Kazak, L., Pollak, M., Mallette, F., Topisirovic, I., & Hulea, L. (2019). mTOR as a central regulator of lifespan and aging. *F1000Research*, *8*, F1000 Faculty Rev-998.

Palmieri, M., Impey, S., Kang, H., di Ronza, A., Pelz, C., Sardiello, M., & Ballabio, A. (2011). Characterization of the CLEAR network reveals an integrated control of cellular clearance pathways. *Human molecular genetics*, *20*(19), 3852–3866.

Parenti, G., Andria, G., & Ballabio, A. (2015). Lysosomal storage diseases: from pathophysiology to therapy. *Annual review of medicine*, *66*, 471–486.

Parrinello, S., Samper, E., Krtolica, A., Goldstein, J., Melov, S., & Campisi, J. (2003). Oxygen sensitivity severely limits the replicative lifespan of murine fibroblasts. *Nature cell biology*, *5*(8), 741–747.

Perera, R. M., & Zoncu, R. (2016). The Lysosome as a Regulatory Hub. *Annual review of cell and developmental biology*, *32*, 223–253.

Pellegrini, R. (2016). Edit single bases with Benchling! https://blog.benchling.com/2016/07/18/base-editor. Accessed 18 July 2016

Pu, J., Guardia, C. M., Keren-Kaplan, T., & Bonifacino, J. S. (2016). Mechanisms and functions of lysosome positioning. *Journal of cell science*, *129*(23), 4329–4339.

Pu, J., Schindler, C., Jia, R., Jarnik, M., Backlund, P., & Bonifacino, J. S. (2015). BORC, a multisubunit complex that regulates lysosome positioning. *Developmental cell*, *33*(2), 176–188.

Ran, F. A., Hsu, P. D., Wright, J., Agarwala, V., Scott, D. A., & Zhang, F. (2013). Genome engineering using the CRISPR-Cas9 system. *Nature protocols, 8*(11), 2281–2308.

Reddy, K., Cusack, C. L., Nnah, I. C., Khayati, K., Saqcena, C., Huynh, T. B., Noggle, S. A., Ballabio, A., & Dobrowolski, R. (2016). Dysregulation of Nutrient Sensing and CLEARance in Presenilin Deficiency. *Cell reports, 14*(9), 2166–2179.

Rezende, E. L., Gomes, F. R., Chappell, M. A., & Garland, T., Jr (2009). Running behavior and its energy cost in mice selectively bred for high voluntary locomotor activity. *Physiological and biochemical zoology: PBZ*, *82*(6), 662–679.

Rosa-Ferreira, C., & Munro, S. (2011). Arl8 and SKIP act together to link lysosomes to kinesin-1. *Developmental cell*, *21*(6), 1171–1178.

Saitoh, S. I., Saitoh, Y. M., Kontani, K., Sato, K., & Miyake, K. (2019). ADP-ribosylation factor-like 8b is required for the development of mouse models of systemic lupus erythematosus. *International immunology*, *31*(4), 225–237.

Saxton, R. A., & Sabatini, D. M. (2017). mTOR Signaling in Growth, Metabolism, and Disease. *Cell*, *168*(6), 960–976.

Settembre, C., Fraldi, A., Medina, D. L., & Ballabio, A. (2013). Signals from the lysosome: a control centre for cellular clearance and energy metabolism. *Nature reviews*. *Molecular cell biology*, *14*(5), 283–296.

Shen, H. M., & Mizushima, N. (2014). At the end of the autophagic road: an emerging understanding of lysosomal functions in autophagy. *Trends in biochemical sciences, 39*(2), 61–71.

Sou, Y. S., Waguri, S., Iwata, J., Ueno, T., Fujimura, T., Hara, T., Sawada, N., Yamada, A., Mizushima, N., Uchiyama, Y., Kominami, E., Tanaka, K., & Komatsu, M. (2008). The Atg8 conjugation system is indispensable for proper development of autophagic isolation membranes in mice. *Molecular biology of the cell, 19*(11), 4762–4775.

Steinman, H. A., Sluss, H. K., Sands, A. T., Pihan, G., & Jones, S. N. (2004). Absence of p21 partially rescues Mdm4 loss and uncovers an antiproliferative effect of Mdm4 on cell growth. *Oncogene*, *23*(1), 303–306.

Sun, H., Gulbagci, N. T., & Taneja, R. (2007). Analysis of growth properties and cell cycle regulation using mouse embryonic fibroblast cells. *Methods in molecular biology (Clifton, N.J.)*, *383*, 311–319.

Takada, T., Mita, A., Maeno, A., Sakai, T., Shitara, H., Kikkawa, Y., Moriwaki, K., Yonekawa, H., & Shiroishi, T. (2008). Mouse inter-subspecific consomic strains for genetic dissection of quantitative complex traits. *Genome research*, *18*(3), 500–508.

Takahashi, A., Kato, K., Makino, J., Shiroishi, T., & Koide, T. (2006). Multivariate analysis of temporal descriptions of open-field behavior in wild-derived mouse strains. *Behavior genetics, 36*(5),

Tarr, B. A., Kellaway, L. A., St Clair Gibson, A., & Russell, V. A. (2004). Voluntary running distance is negatively correlated with striatal dopamine release in untrained rats. *Behavioural brain research*, *154*(2), 493–499.

Turri, M. G., Datta, S. R., DeFries, J., Henderson, N. D., & Flint, J. (2001). QTL analysis identifies multiple behavioral dimensions in ethological tests of anxiety in laboratory mice. *Current biology*, *11*(10), 725–734.

Umemori, J., Nishi, A., Lionikas, A., Sakaguchi, T., Kuriki, S., Blizard, D. A., & Koide, T. (2009). QTL analyses of temporal and intensity components of home-cage activity in KJR and C57BL/6J strains. *BMC genetics*, *10*, 40.

Wu, Y. E., Huo, L., Maeder, C. I., Feng, W., & Shen, K. (2013). The balance between capture and dissociation of presynaptic proteins controls the spatial distribution of synapses. *Neuron*, *78*(6), 994–1011.

de Visser, L., van den Bos, R., & Spruijt, B. M. (2005). Automated home cage observations as a tool to measure the effects of wheel running on cage floor locomotion. *Behavioural brain research*, *160*(2), 382–388.

Yang, H. S., Shimomura, K., Vitaterna, M. H., & Turek, F. W. (2012). High-resolution mapping of a novel genetic locus regulating voluntary physical activity in mice. *Genes, brain, and behavior, 11*(1), 113–124.

Yoshii, S. R., Kuma, A., Akashi, T., Hara, T., Yamamoto, A., Kurikawa, Y., Itakura, E., Tsukamoto, S., Shitara, H., Eishi, Y., & Mizushima, N. (2016). Systemic Analysis of Atg5-Null Mice Rescued from Neonatal Lethality by Transgenic ATG5 Expression in Neurons. *Developmental cell, 39*(1), 116–130.

Name	sequence (5' to 3')	Length (nt)	Chr.	Strand	Start	End	Experiment
mArl8b-ex2-small-F	TAAGTGCCTCCCAACTCCAA	20	6	+	108813476	108813495	Genotyping
mArl8b-ex2-small-R	TGCATGCATGTACGCAGAC	19	6	-	108813853	108813872	
Arl8b_GDP_form_F2	TGTTGACATGCGTTTGCTGG	20	6	+	108782836	108782855	
Arl8b-GDP-form-R	CGTGGAATTGACCCTCCTGC	20	6	-	108783493	108783512	
Arl8b-GTP- form-F2	CCATGATTGAAATGTGCTGGC	21	6	+	108814728	108814748	
Arl8b-GTP- form-R2	CTCCAGGGATACCAAGACGG	20	6	-	108815411	108815430	
mArl8b-ex2-gRNA-Fmod	GGATCCTAATACGACTCACTATAGGGCATATCTTCACTGAATTGACGTTTTAGAGCTAGAAATAGC	66					CRISPR/Cas9
T7- Arl8b-GTP-gRNA-2ndPCR-F	GGATCCTAATACGACTCACTATAGGGAGTACCGCTCCCACATGCTCGTTTTAGAGCTAGAAATAGC	66					
T7- Arl8b-GTP-gRNA-2ndPCR-F2	GGATCCTAATACGACTCACTATAGGGGGGACATAGGCGGACAGCCCGTTTTAGAGCTAGAAATAGC	66					
T7- Arl8b-GDP-gRNA-2ndPCR-F	GGATCCTAATACGACTCACTATAGGGAGATGGAACTGACGCTCGTGGTTTTAGAGCTAGAAATAGC	66					
T7- Arl8b-GDP-gRNA-2ndPCR-F2	GGATCCTAATACGACTCACTATAGGGATTGACGAAGGTGGTCTTGCGTTTTAGAGCTAGAAATAGC	66					
T7- Arl8b-GDP-gRNA-2ndPCR-F3	GGATCCTAATACGACTCACTATAGGGCACCGCGATGACATTGACGAGTTTTAGAGCTAGAAATAGC	66					
Arl8b-GTP- form-oligo3	AACTGCCTTGTTTTCATTAAAGATCTGGGACATAGGCGGACTGCCCCGGTTTCGGAGCATGTGGGAGCGGTACT GCCGAG	80					
Arl8b-GTP- form-oligo4	AACTGCCTTGTTTTCATTAAAGATCTGGGACATAGGCGGACTGCCCCGCTTCCGGAGCATGTGGGAGCGGTACTGCCGAG	80					
Arl8b-GDP-form-oligo	TTCGCTCTTCTGGAAGGAGGAGATGGAACTGACGCTCGTGGGGCTGCAGTACTCCGGCAAGAACACCTTCGTCAATGTCA	80					
Arl8b-GDP-form-oligo2	GATGGAACTGACGCTCGTGGGGCTGCAGTACTCCGGCAAGAACACCTTCGTCAATGTCATCGCGGTGAGCAGCCCTCTGC	80					

Table.1 Summary of primer and oligonucleotide sequences

(A) *Arl8b*-KO

Stage	Total no. of embryos or mice examined	No. with genotype			Total no. of litters examined	Survival of *Arl8b*$^{-/-}$ embryos (%)
		Arl8b$^{+/+}$	*Arl8b*$^{+/-}$	*Arl8b*$^{-/-}$		
Embryonic						
E15.5	119	40	59	20	15	16.8
E18.5	71	15	35	21	14	29.6
Postnatal (3-4 week old)	18	10	8	0	26	0

(B) *Arl8b*$^{\Delta 9}$

Stage	Total no. of embryos or mice examined	No. with genotype			Total no. of litters examined	Survival of *Arl8b*$^{\Delta 9/\Delta 9}$ embryos (%)
		Arl8b$^{+/+}$	*Arl8b*$^{+/\Delta 9}$	*Arl8b*$^{\Delta 9/\Delta 9}$		
Embryonic						
E15.5	89	27	45	17	21	19.1
E18.5	92	24	52	16	11	17.4
Postnatal (3-4 week old)	83	35	48	0	5	0

(C) *Arl8b*^{Q75L}

Stage	Total no. of embryos or mice examined	No. with genotype			Total no. of litters examined	Survival of *Arl8b*$^{Q75L/Q75L}$ embryos (%)
		Arl8b$^{+/+}$	*Arl8b*$^{+/Q75L}$	*Arl8b*$^{Q75L/Q75L}$		
Embryonic						
E15.5	32	10	15	7	5	21.9
E18.5	34	6	21	7	5	20.6
Postnatal (3-4 week old)	33	10	19	4	7	12.1

(D) *Arl8b*^{T34N}

Stage	Total no. of embryos or mice examined	No. with genotype			Total no. of litters examined	Survival of *Arl8b*$^{T34N/T34N}$ embryos (%)
		Arl8b$^{+/+}$	*Arl8b*$^{+/T34N}$	*Arl8b*$^{T34N/T34N}$		
Embryonic						
E15.5	47	14	22	11	10	23.4
E18.5	23	8	11	4	4	17.4
Postnatal (3-4 week old)	36	17	19	0	5	0

Table 2. Genotype analyses of progeny from crossing heterozygous mice for *Arl8b*$^{+/-}$(A), *Arl8b*$^{+/\Delta 9}$ (B), GTP-binding form mutant *Arl8b*$^{+/Q75L}$ (C) and GDP-binding form mutant *Arl8b*$^{+/T34N}$ (D), respectively. All embryos were genotyped using the tail samples.

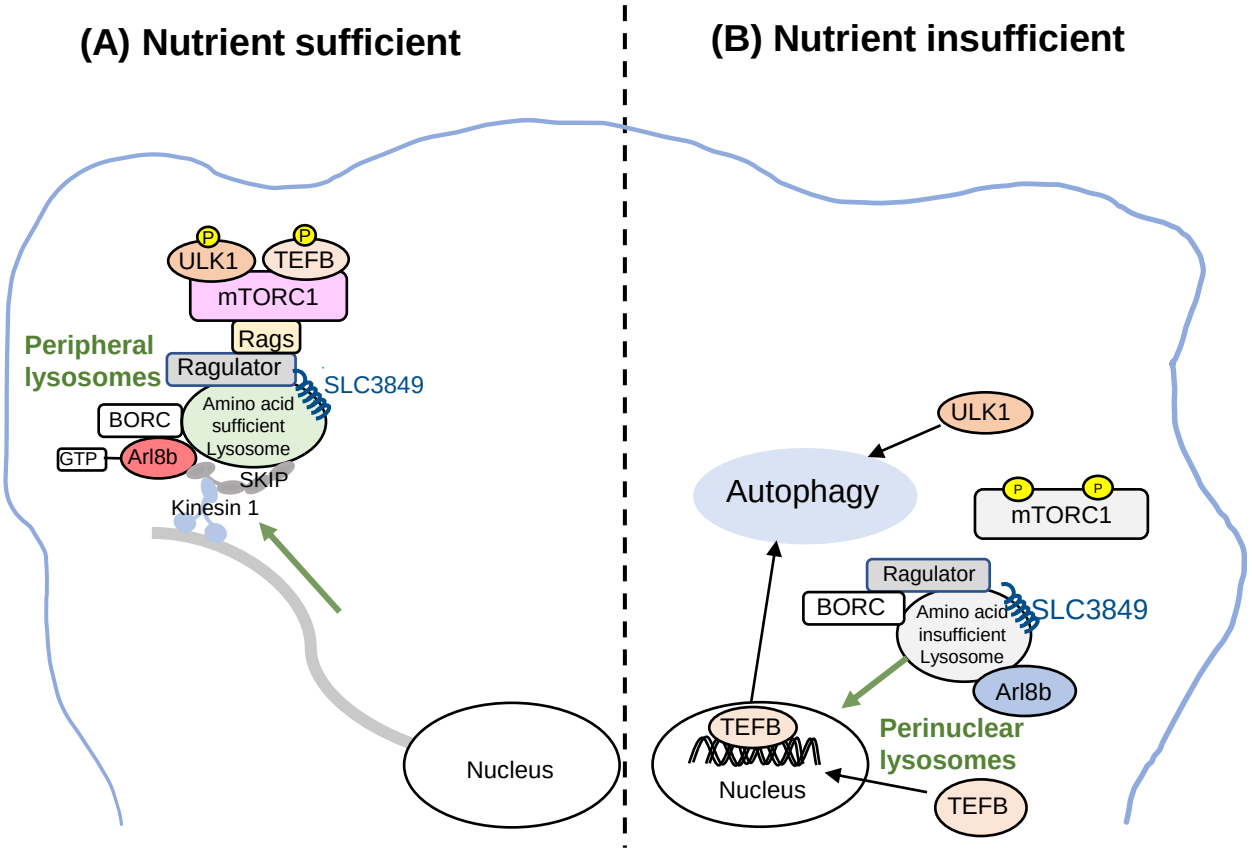

Figure 1.Nutrient-activated mTORC1 in peripheral lysosomes
mTORC1 signaling under nutrient-sufficient status (A) and nutrient-insufficient status (B).

(A) In nutrient-sufficient status, amino acids are transported to the cytoplasmic side of lysosomal membranes by a transporter SLC38A9, an arginine-regulated transporter of major amino acids. In the presence of lysosomal amino acids, SLC38A9 activates a lysosomal molecular complex Ragulator, which recruits and activates mTORC1 to lysosomes. Simultaneously, Ragulator releases BLOC-one-related (BORC) complex, and the released BORC complex recruits Arl8b and SKIP, resulting in transport of lysosomes to the cell peripherally. Accordingly, the peripheral lysosome is a platform for activation of mTORC1 signaling.

(B) Under nutrient-deprived condition, SLC38A9 is unable to bind to Ragulator resulting in releasing mTORC1 from lysosomes. Subsequently, the released Ragulator associates with BORC complex and inhibits Arl8b-dependent lysosomal movement toward the cell peripherally. Therefore, nutritionally deficient lysosomes are distributed in the perinuclear region. In parallel, the released mTORC1 becomes inactivated, resulting in decreased phosphorylation of two key substrates: the autophagy-initiating UNC51-like kinase 1 (ULK1) and the transcription factor EB (TFEB). Dephosphorylated ULK1 is released from lysosomes and promotes the formation of the phagophore, which is a precursor of the autophagosome. Dephosphorylated TFEB transfers lysosomes to the nucleus to upregulate the expression of autophagy-associated genes.

These schemes are based on findings in previous studies (Shen et al.2014; Reddy et al. 2016; Dossou et al. 2019; Miyake et al. 2019).

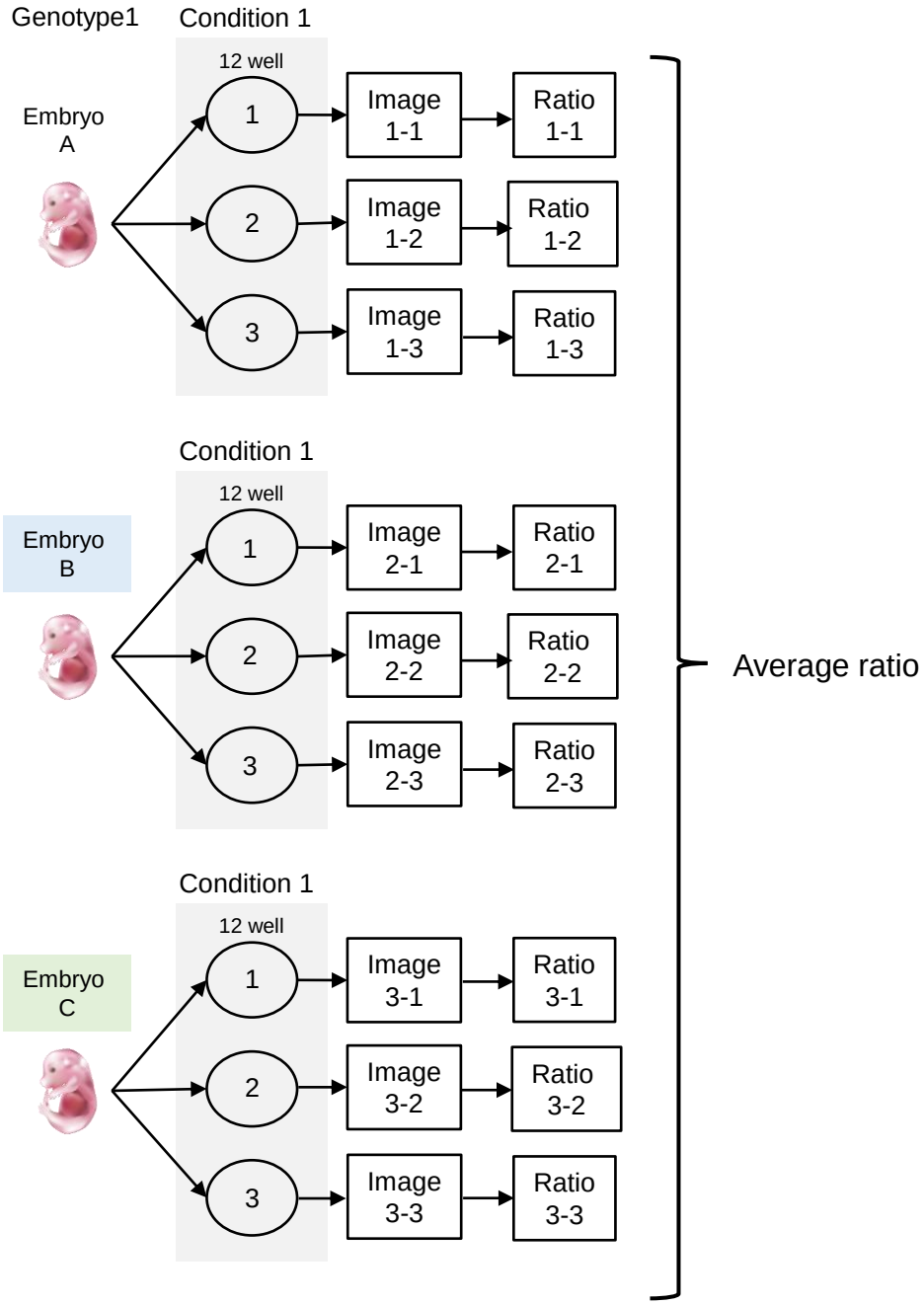

Figure 2. Experimental design for lysosome positioning in response to nutrient availability. For one condition, three embryos from the same genotype were used in triplicates. From each experiment, three images and three ratios were obtained. Totally, nine ratios were calculated per genotype. The average ratio were calculated from nine ratios.

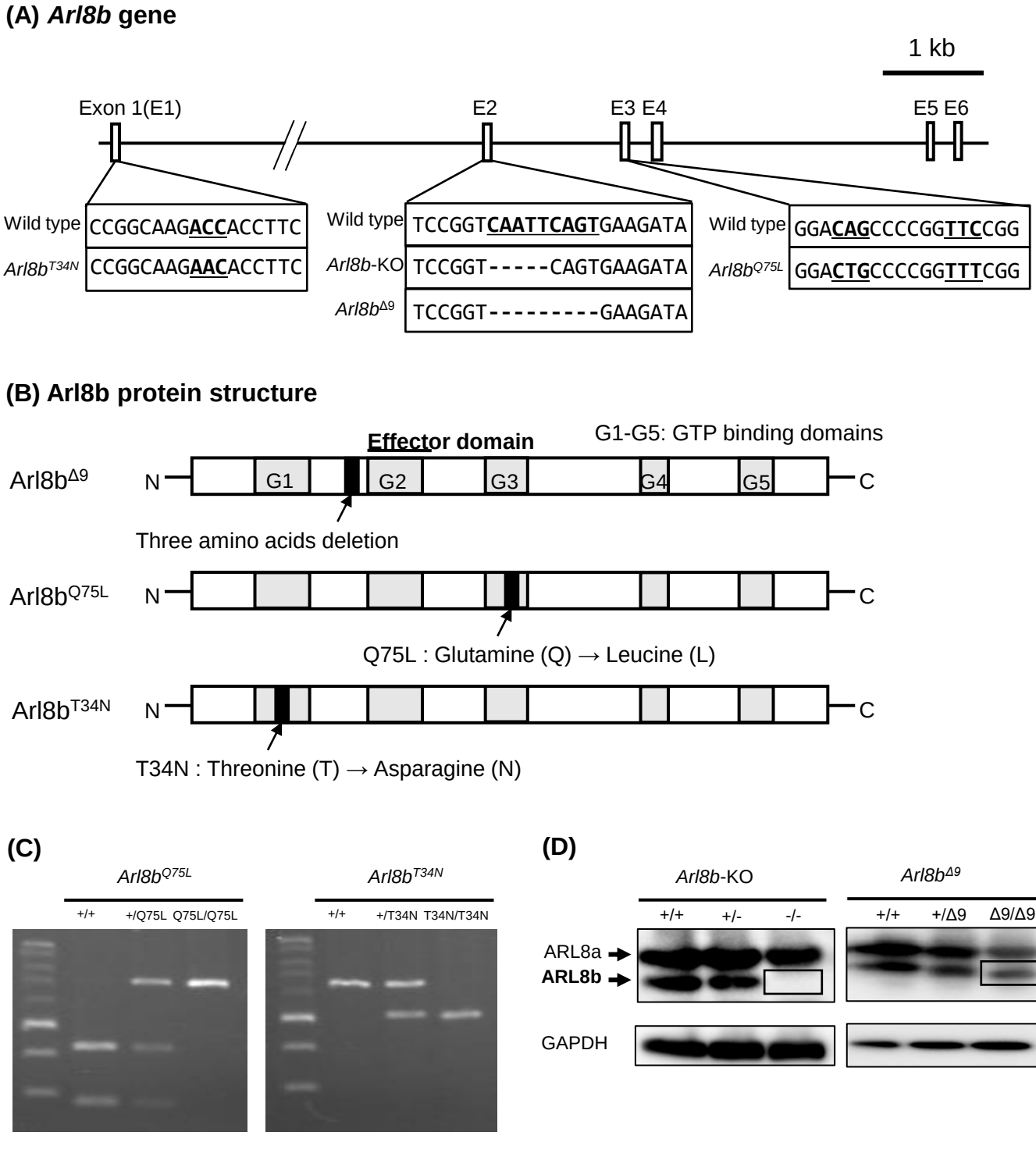

Figure 3. Generation of *Arl8b* gene-edited mutants.

(A) Schematic diagram of *Arl8b* gene. Mutants were obtained by using CRISPR/Cas9 genome editing technique. *Arl8b*$^{\Delta 9}$ mutants have deletions of 9 base pairs in exon 2 of *Arl8b* gene and *Arl8b*-KO have the deletions of 5 base pairs, respectively. GTP-bound form mutant *Arl8b*^{Q75L} have a nonsynonymous SNP in exon 1, and GDP-bound form mutant *Arl8b*^{T34N} have a nonsynonymous SNP in exon 3.

(B) Schematic diagram of Arl8b protein. Arl8b protein contains GTP binding domains (G1 –G5) and the effector domain which is for interacting other proteins. Arrow indicates a mutation of each mutant. In the *Arl8b*$^{\Delta 9}$ mutant, three amino acids were deleted between the GTP binding domains G1 and G2. *Arl8b*^{Q75L} mice have one amino acid substitution in the G3 domain and *Arl8b*^{T34N} mice has one amino acid substitution in the G1 domain.

(C) Restriction enzyme treatment after genotyping PCR of ear genomic DNA. For restriction enzyme treatment, *Nla*VI and *Xmn*I are used for *Arl8b*^{Q75L} and *Arl8b*^{T34N} mutants, respectively.

(D) Western blot analyses of *Arl8b*$^{\Delta 9}$ and *Arl8b*-KO mutants of embryonic brains at E18.5. Arl8b protein expression was detected in homozygote for *Arl8b*$^{\Delta 9}$ mutant.

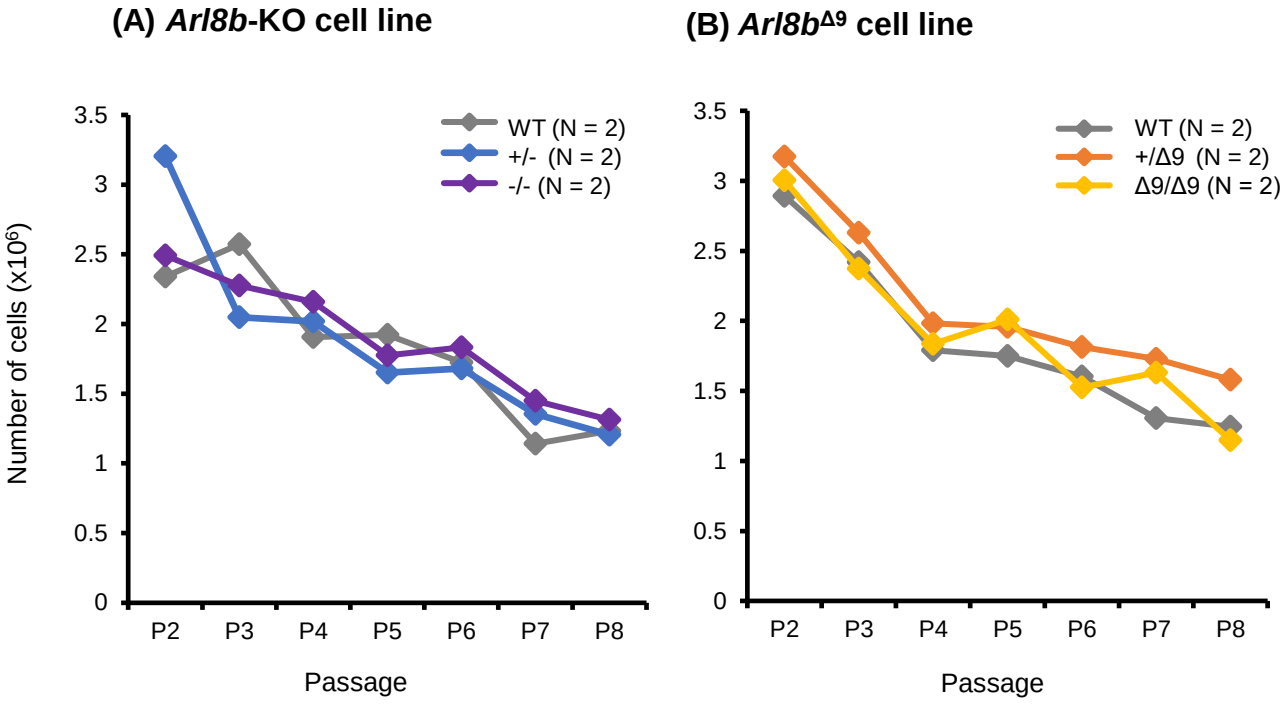

Figure 4. Number of cells over serial passaging according to the 3T3 protocol, carried out in (A) *Arl8b*-KO primary cultured cells and (B) *Arl8b*$^{\Delta 9}$ primary cultured cells. Two biological duplicates per genotypes were assessed.

(A)

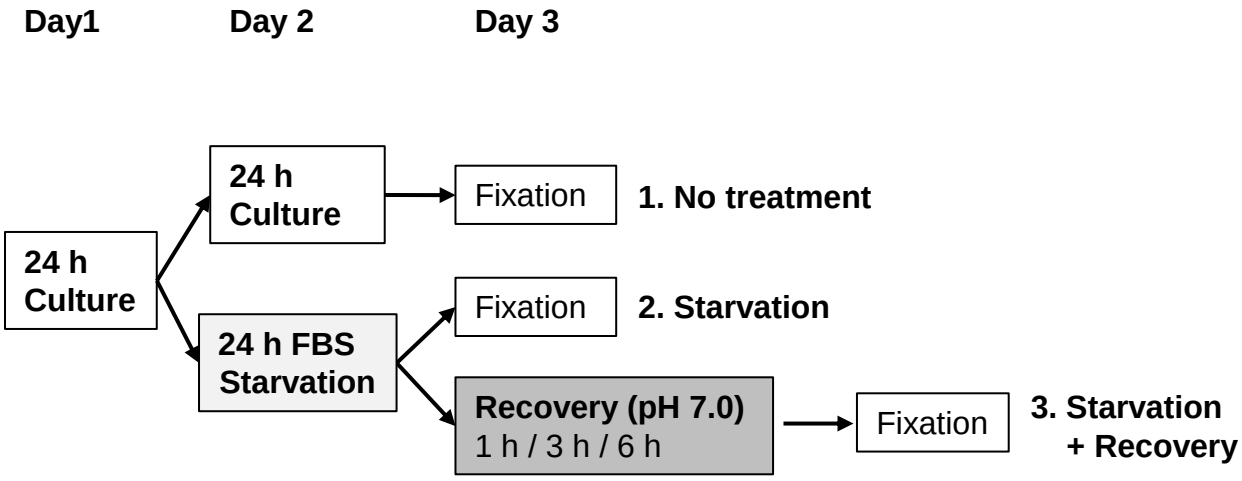

(B)

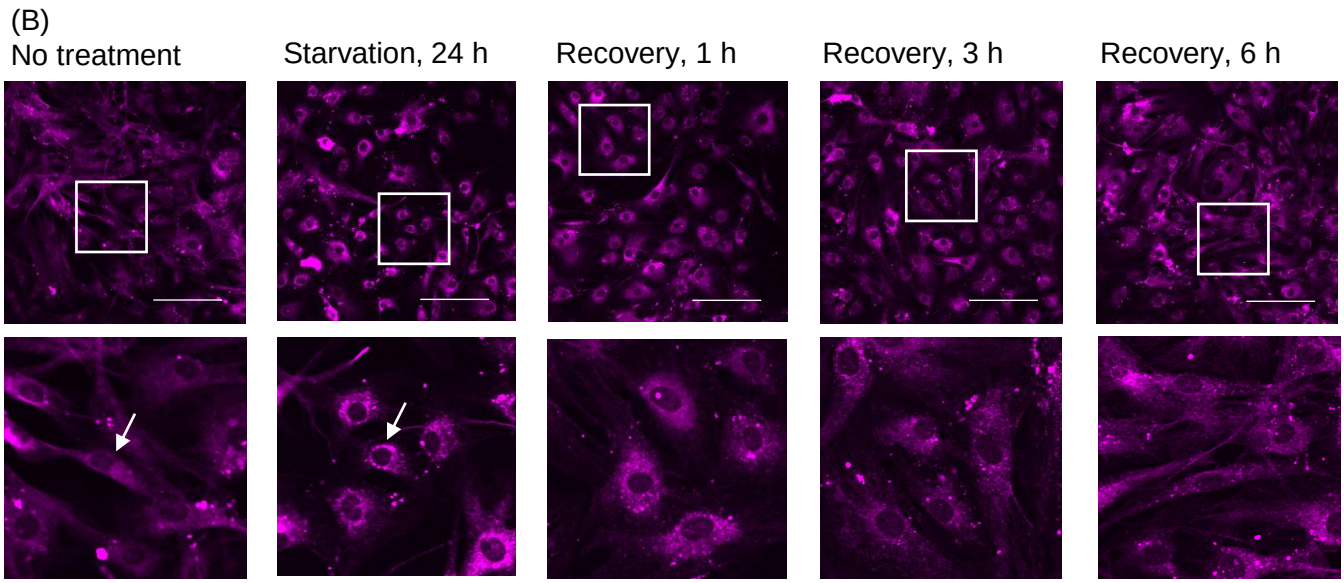

Figure 5. The change of lysosome distribution under different nutritional status in WT MEFs. (A)Timeline for a starvation and a recovery experiment in WT MEFs. After 24 h culture, MEF cells were divided into three groups: no treatment group, starvation group and recovery group. No treatment group were fixed after another 24 h culture under normal condition. For starvation and recovery group, FBS starvation for 24 h were performed. After 24 h FBS starvation, starvation group were fixed. Recovery group were added recovery medium after starvation and fixed after 1 h, 3 h, 6 h, respectively.
(B-F)Representative images of control MEFs under 5 conditions: no treatment, FBS starvation for 24h, recovery treatment for 1 h, 3 h, 6 h. Bottom images are high-magnification images of upper images. Arrow in no treatment group indicates a representative cell with predominantly peripheral lysosomes. Arrow in the starvation group indicates a representative cell with predominantly perinuclear lysosomes. Bar, 200 ㎛.

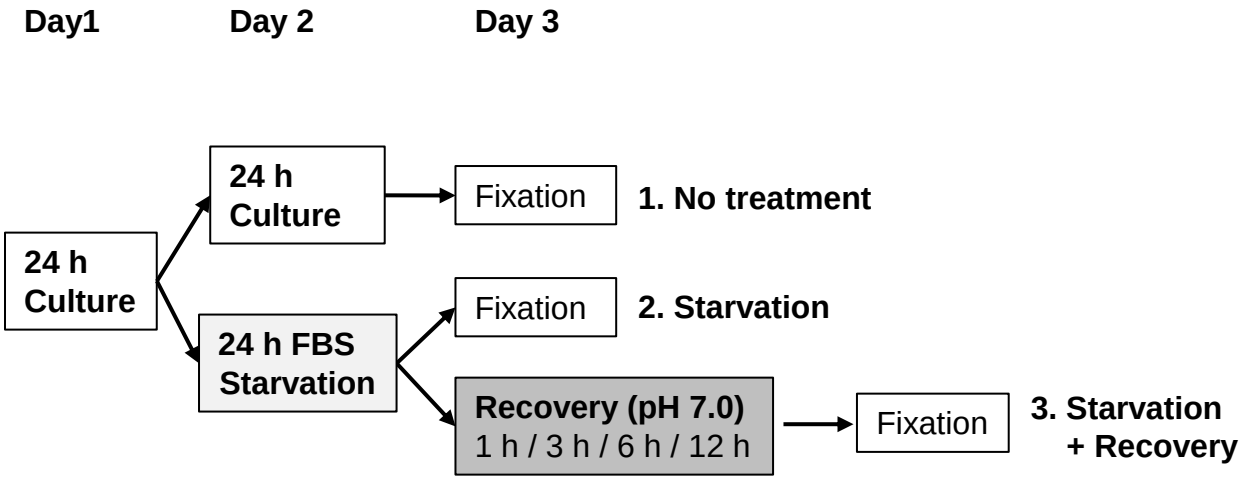

Figure 6. Timeline for starvation and recovery experiment in MEFs from *Arl8b* gene-edited mutant MEFs.
After 24 h culture, MEF cells were divided into three groups: no treatment group, starvation group and recovery group. No treatment group were fixed after another 24 h culture under a normal condition. For starvation and recovery group, FBS starvation for 24 h were performed. After 24 h FBS starvation, starvation group were fixed. Recovery group were added recovery medium after starvation and fixed after 1 h, 3 h, 6 h and 12 h, respectively.

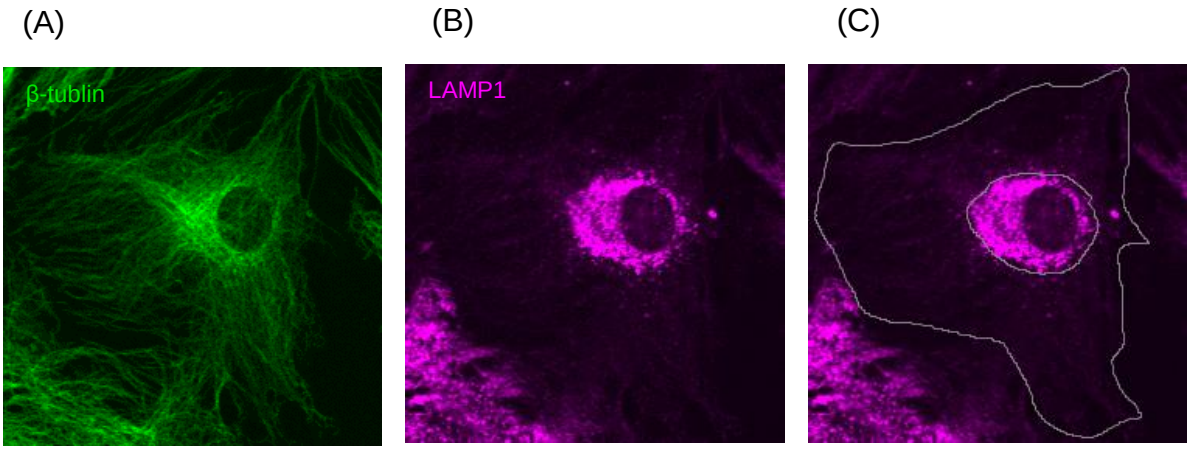

Figure 7. Quantification of lysosomal distribution by ROI manager tool in Image J.
(A) A representative cytoskeleton image by β-tublin staining. (B) The representative image by LAMP1 staining which is used the same image of (A). (C) Gray line is the outline of the whole cell body area and the lysosome detected area. Outer enclosing line represents the whole cell body area. Inner enclosing line represents lysosome detected area.

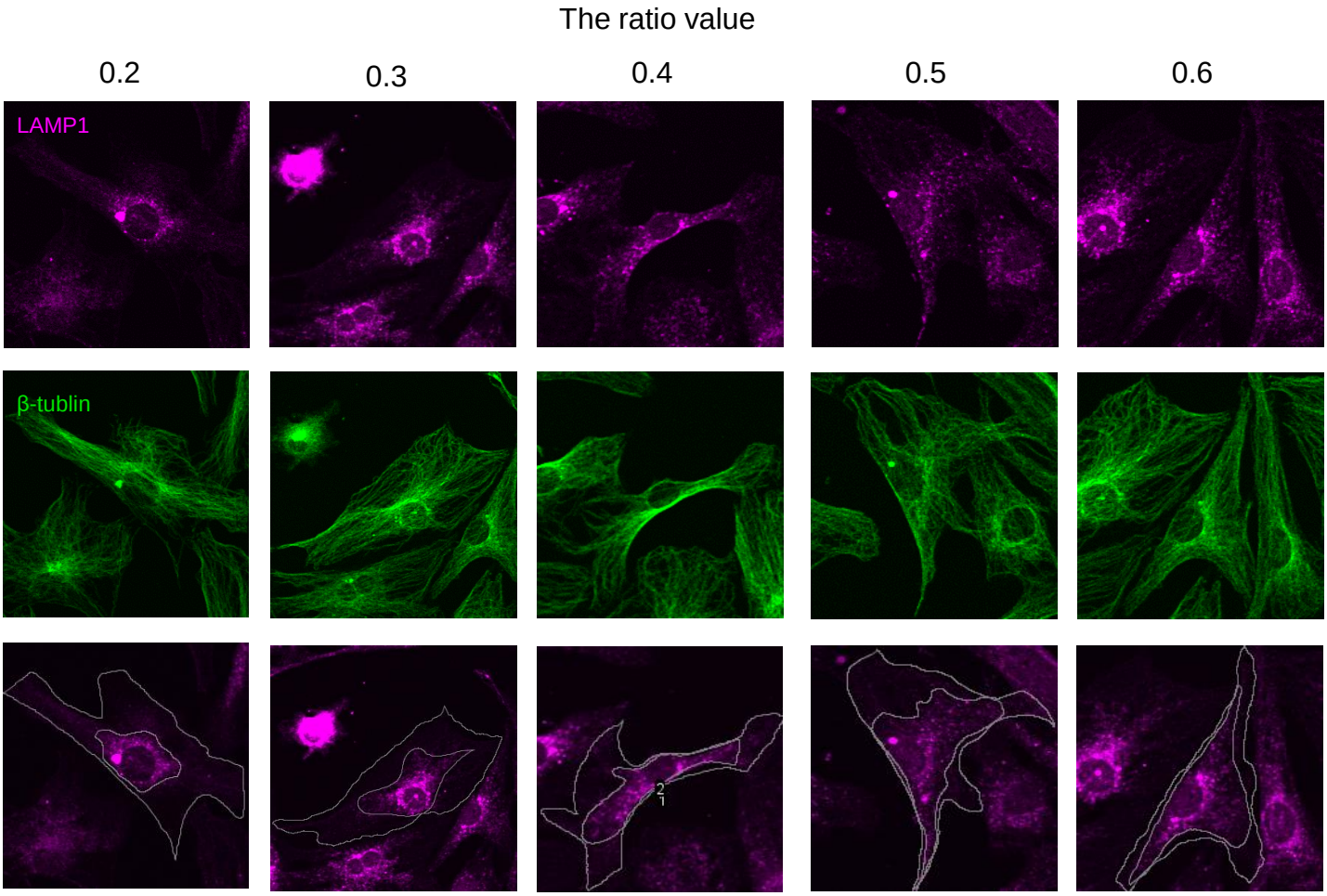

Figure 8. Representative images of MEFs according to the ratio value (lysosome detected area / whole cell body area) from 0.2 to 0.6.
Upper images show lysosome distribution by LAMP1-staining. Middle images show cytoskeleton of the upper images by β-tublin staining. Gray line is the outline of the whole cell body area and the lysosome detected area. Outer enclosing line represents the whole cell body area. Inner enclosing line represents lysosome detected area.

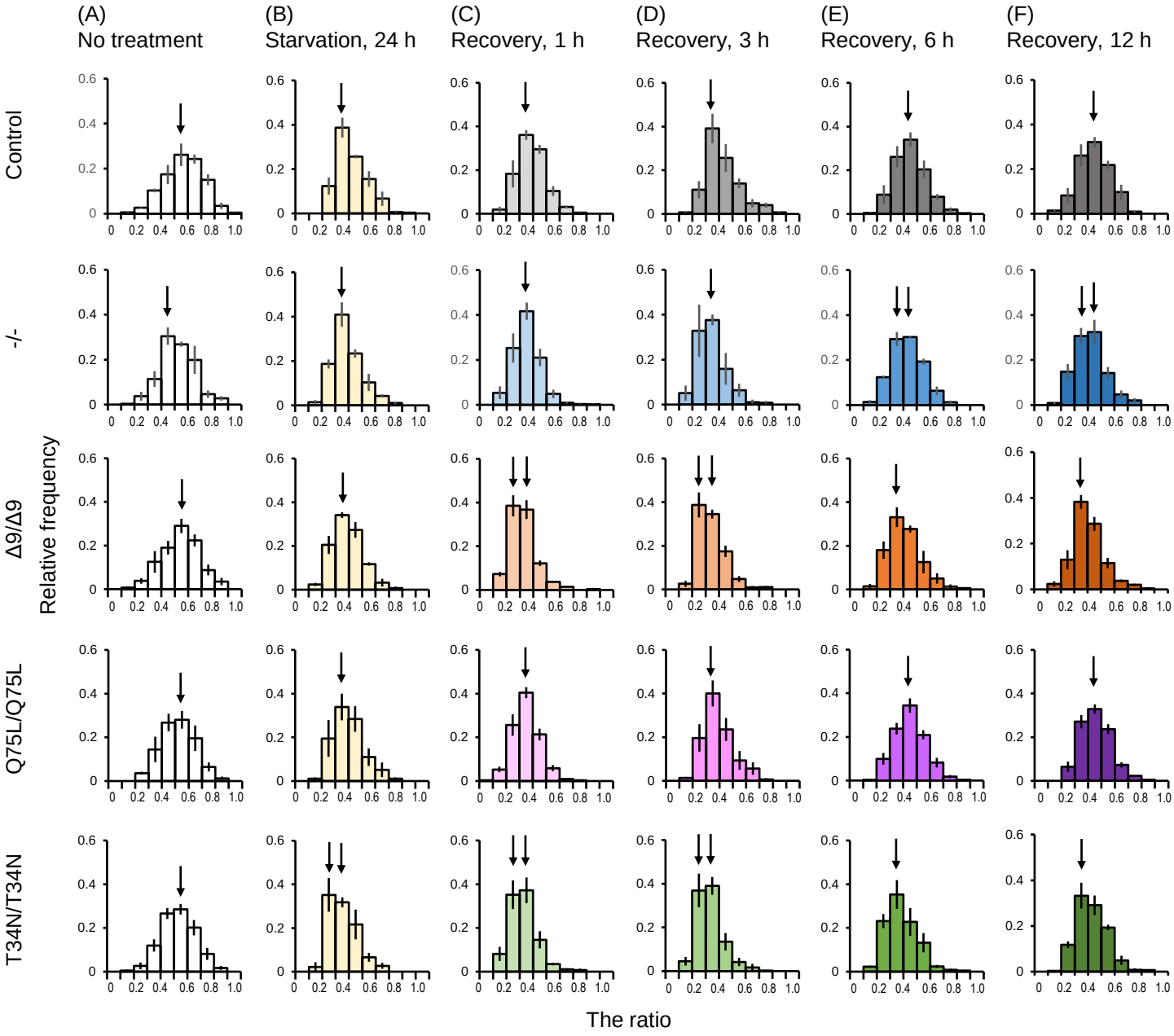

Figure 9. Histogram of lysosome distribution according to the ratio value under 6 conditions: no treatment (A), FBS starvation for 24 h (B), recovery treatment for 1 h (C), 3 h (D), 6 h (E), 12 h (F).
Arrows indicate distribution's peak in each condition. 20 - 50 cells in each image are divided into 10 groups according to their ratio. Three biological replicates carried out in independent experiments in triplicate. Error Bars represent s.e.m.

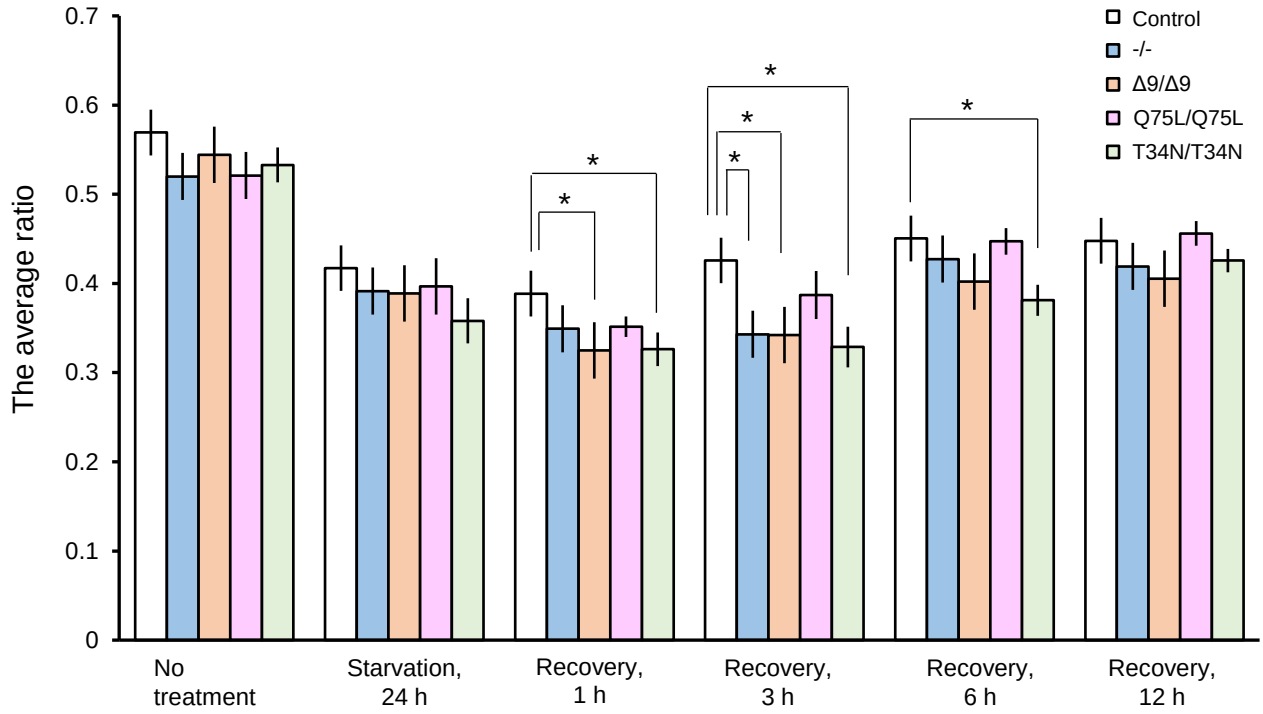

Figure 10. Comparison of the average ratio among genotypes within the same conditions. The average ratio was calculated from three ratios from three different embryos (N = 9). Error Bars represent s.e.m.. *P < 0.05 (Bonferroni / Dunnet test).

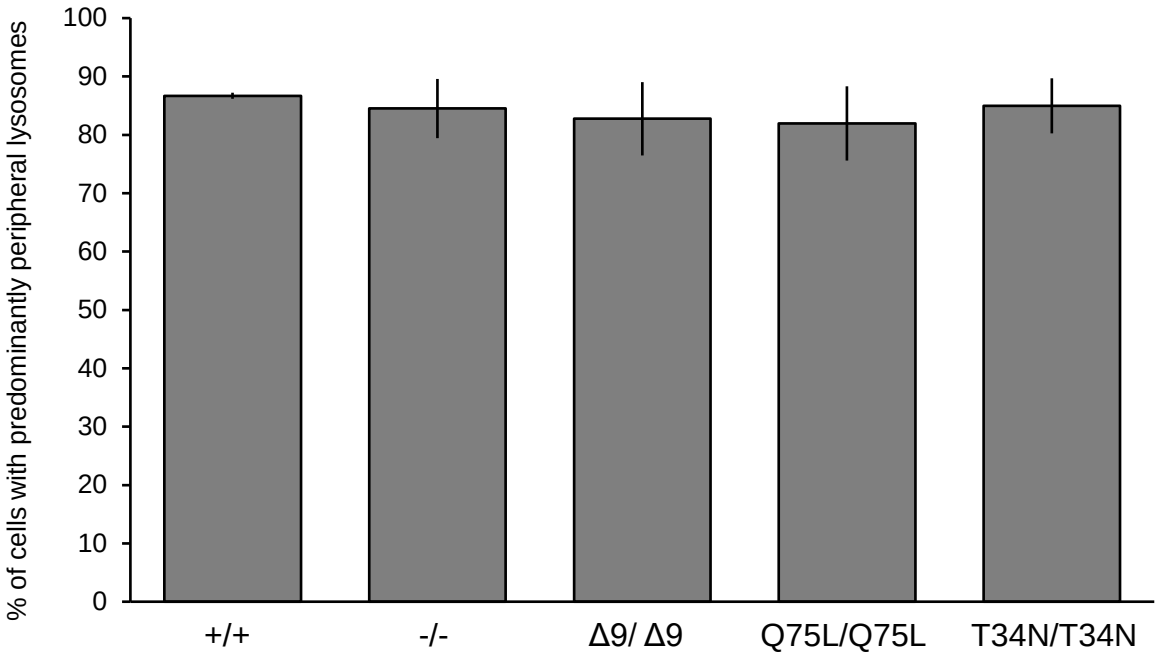

Figure 11. The percentage of cells with predominantly peripheral lysosomes under no treatment condition.
Cells with the ratio more than 0.4 were categorized into cells with peripheral-dominant lysosomal pattern. Cells with the ratio under 0.4 were categorized into cells with perinuclear-dominant lysosomal pattern. The percentage was calculated based on the average of 9 images from 3 different embryos in each strain (N = 9).

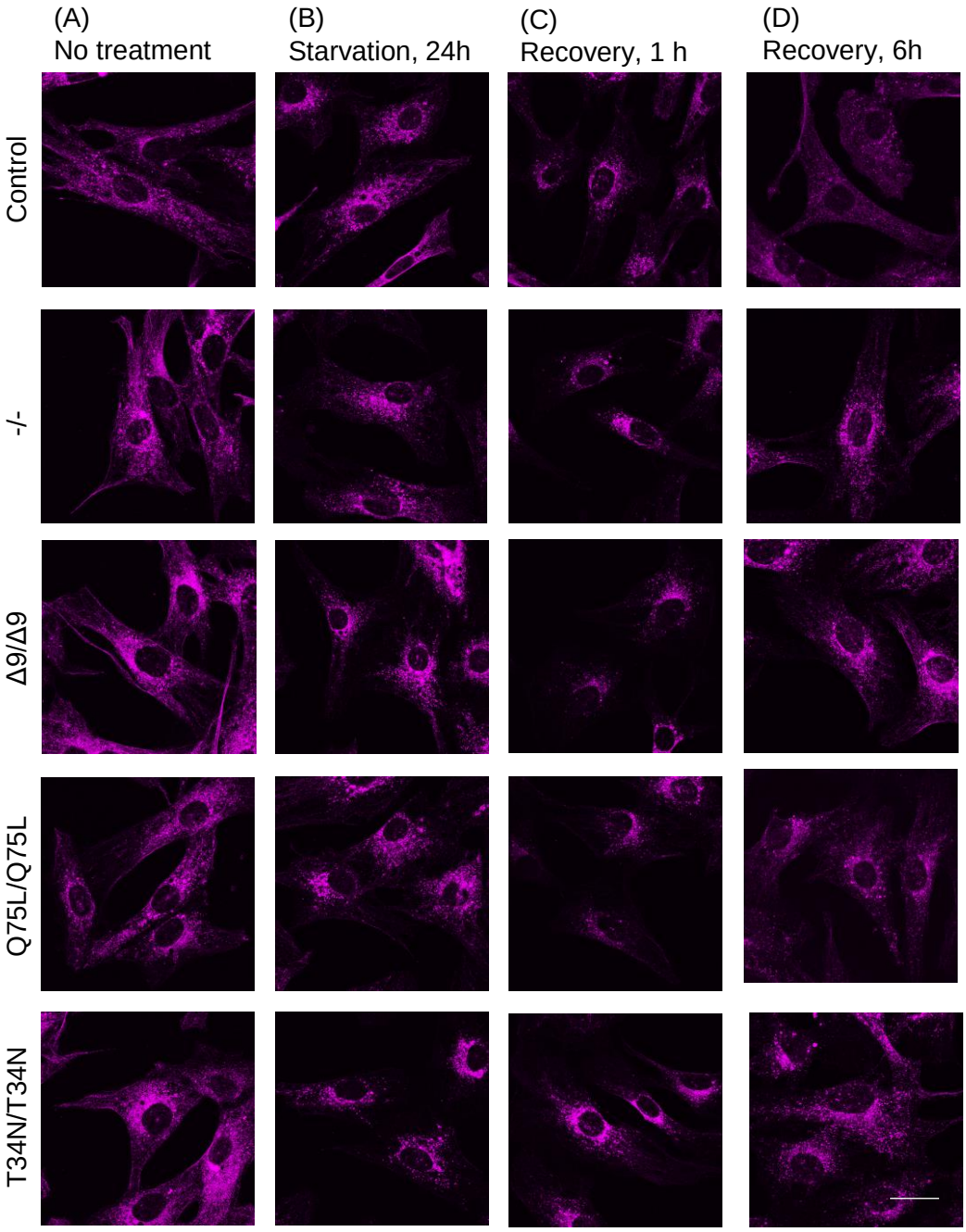

Figure 12. Representative images of lysosomal patten of control and Arl8b mutant MEFs (*Arl8b*$^{-/-}$, *Arl8b*$^{\Delta 9/\Delta 9}$, *Arl8b*$^{Q75L/Q75L}$ and *Arl8b*$^{T34N/T34N}$) among 4 different conditions: no treatment (A), FBS starvation for 24 h (B), recovery treatment for 1 h (C), 6 h (D).
Bar, 30 ㎛.

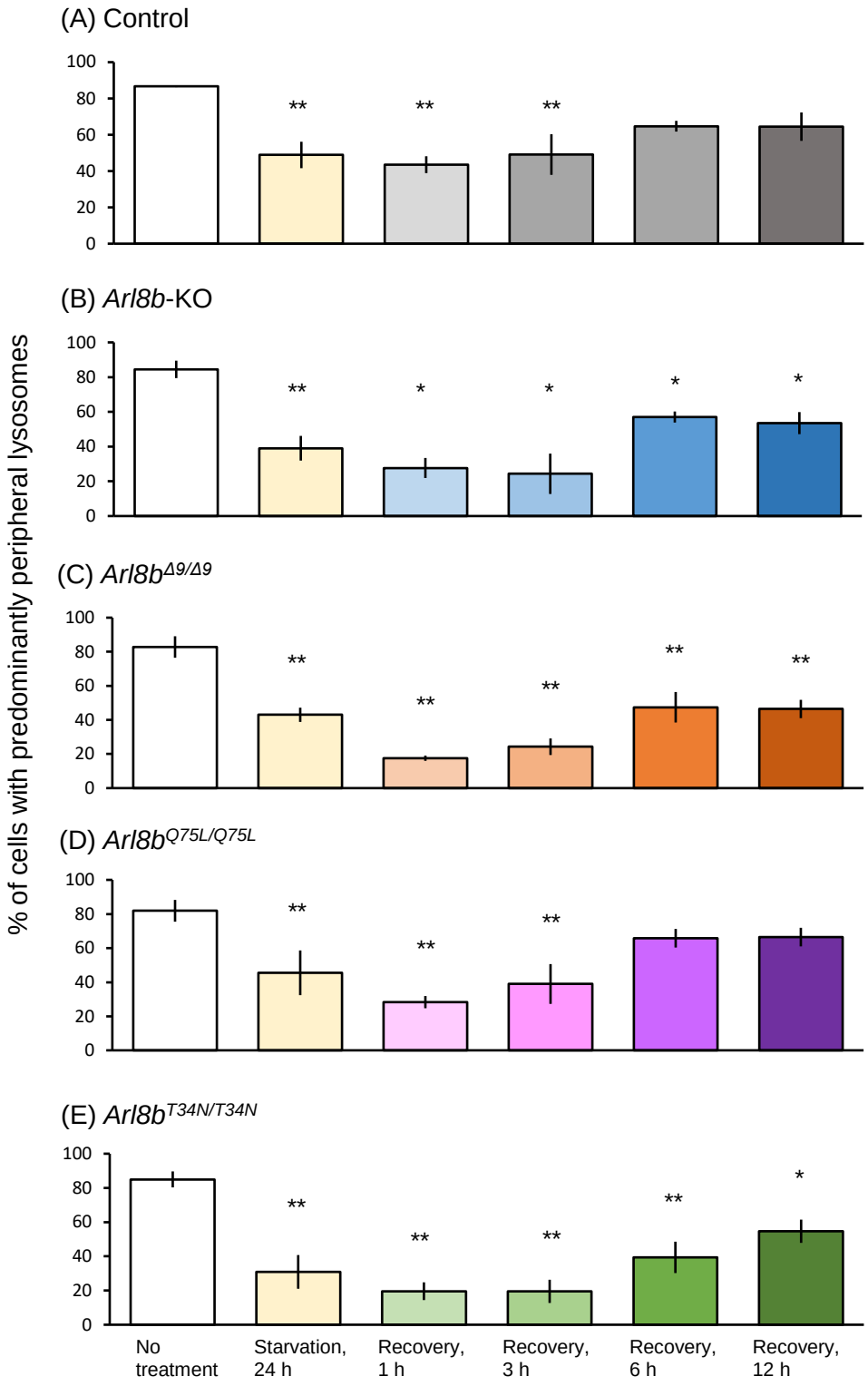

Figure 13. The comparison of lysosomal patten of each strain among different conditions. Statistical analysis was performed within the same genotypes. The average percentage of cells with predominantly peripheral lysosomes of *Arl8b*$^{-/-}$ (A), *Arl8b*$^{\Delta 9/\Delta 9}$ (B), *Arl8b*$^{Q75L/Q75L}$ (C) and *Arl8b*$^{T34N/T34N}$ (D) under different conditions. N = 9. Error Bars represent s.e.m.. *P < 0.05, **P < 0.01 (Bonferroni / Dunnet test).

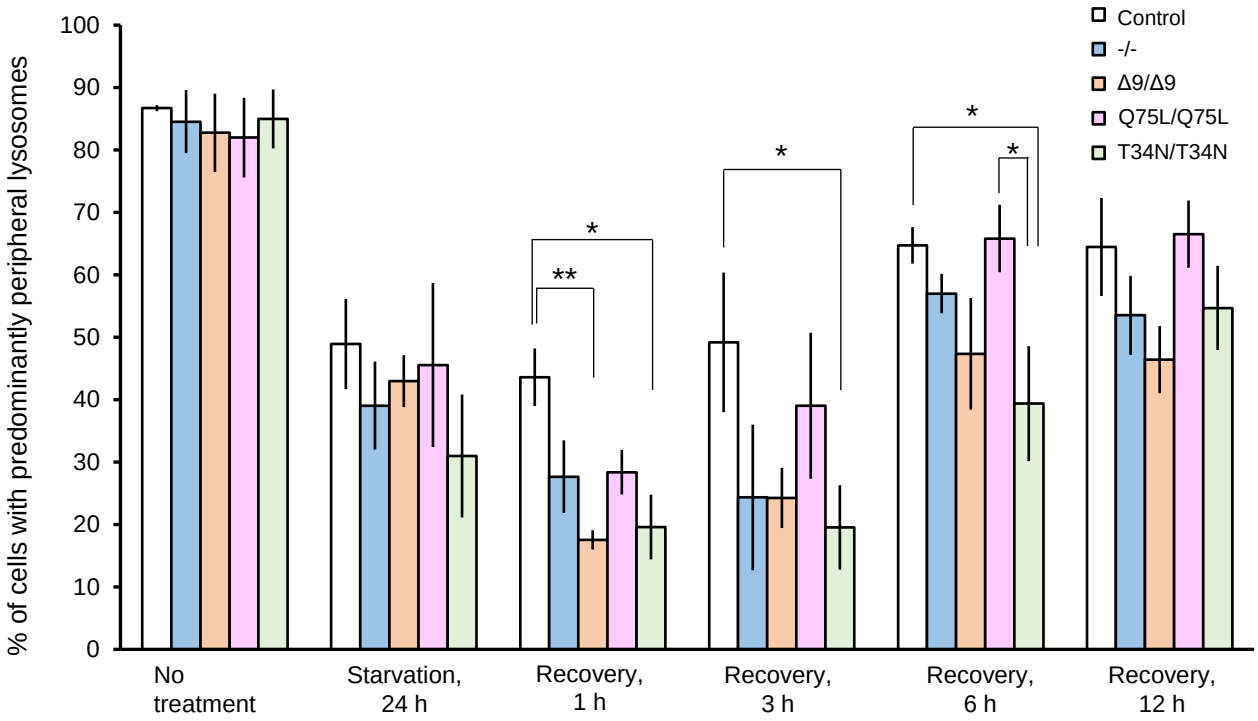

Figure 14. Comparison of lysosomal patten among genotypes within the same conditions. The average ratio was calculated from three ratios from three different embryos (N = 9). Error Bars represent s.e.m.. *P < 0.05 (Bonferroni / Dunnet test).

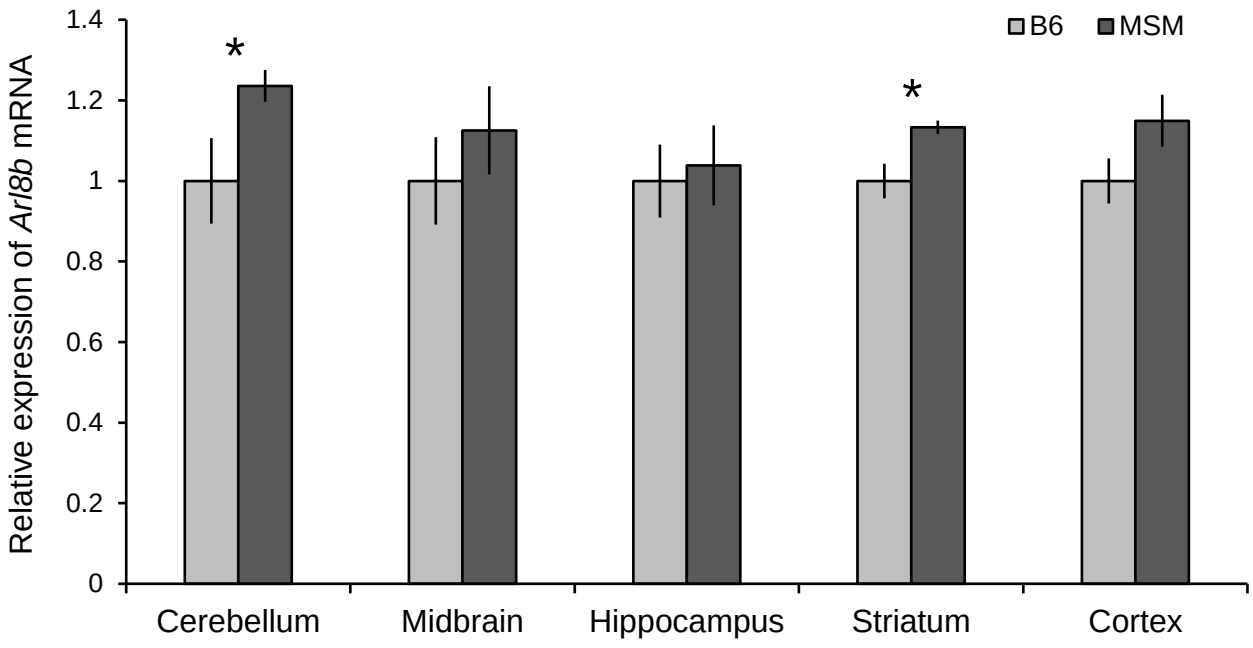

Figure 15. Expression of *Arl8b* gene in five brain tissues: cerebellum, midbrain, hippocampus, striatum and cortex.
Expression was assessed by qRT-PCR, normalizing to β-actin. Relative expression of *Arl8b* gene in cerebellum, midbrain and cortex of B6 and MSM. N=3-5 for each mouse strain. Error Bars represent s.e.m. *P < 0.05 (one-way ANOVA).

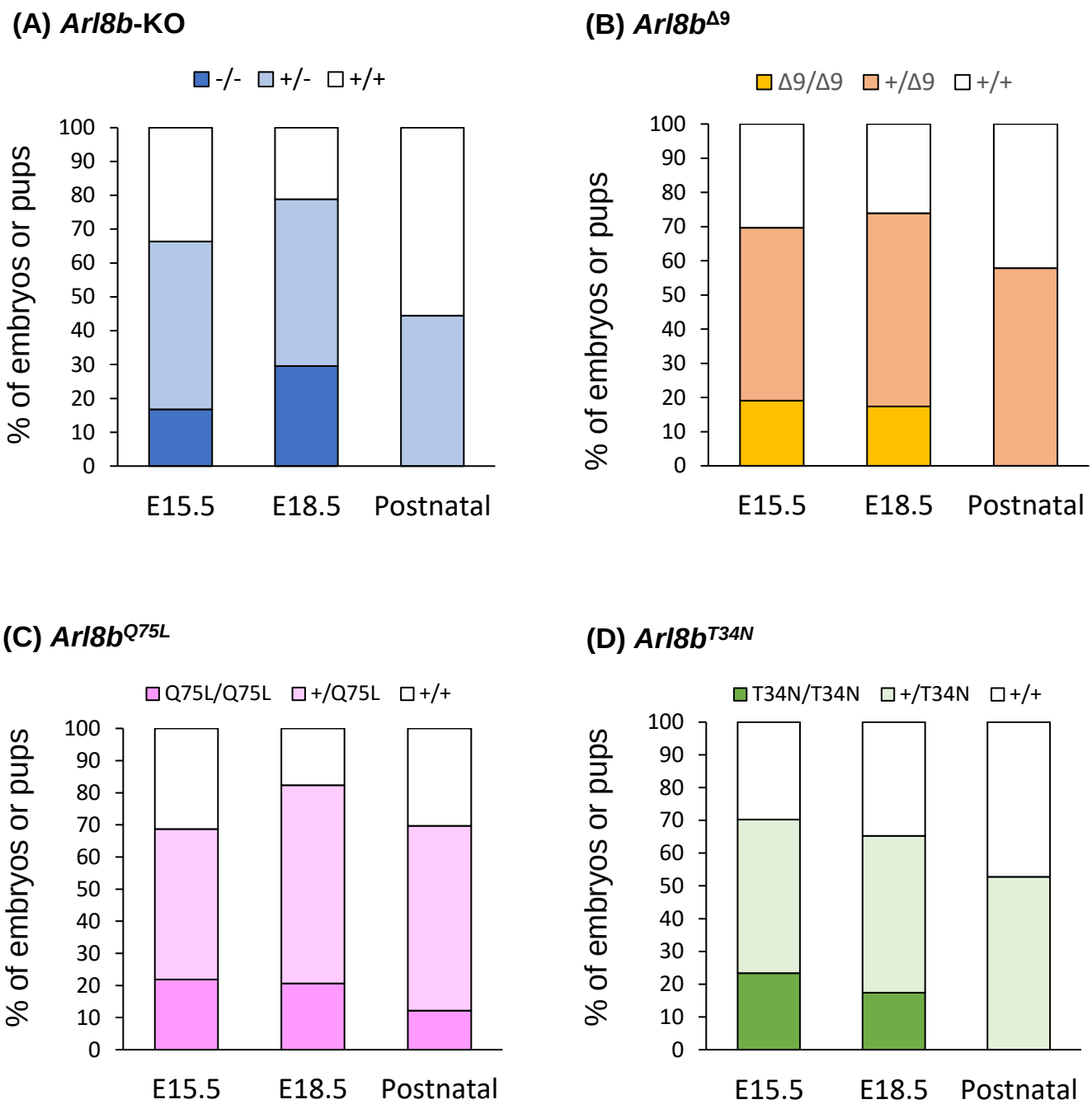

Figure 16. Genotype analyses of progeny from crossing heterozygous mice of *Arl8b*$^{+/-}$(A), *Arl8b*$^{+/\Delta 9}$ (B), *Arl8b*$^{+/Q75L}$ (C) and *Arl8b*$^{+/\ T34N}$ (D), respectively. All embryos were genotyped using the tail samples. The number of embryos and pups examined is listed in Table 2.

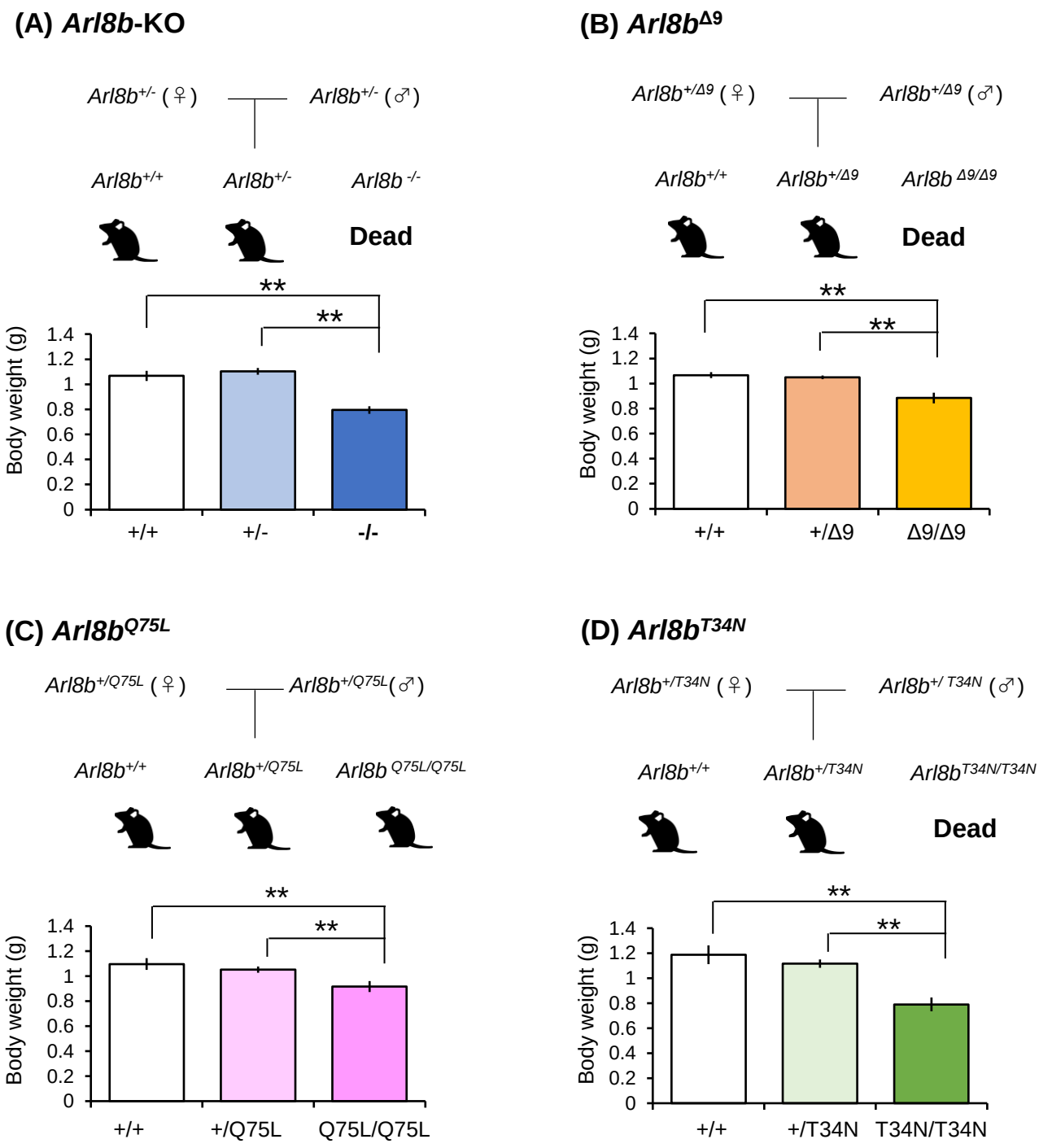

Figure 17. Comparison of body weight at E18.5 among genotypes.
N = 15, 35 and 21 mice for *Arl8b*$^{+/+}$ and *Arl8b*$^{+/-}$, *Arl8b*$^{-/-}$ in *Arl8b*-KO strain, respectively.
N = 26, 32 and 16 mice for *Arl8b*$^{+/+}$ and *Arl8b*$^{+/\Delta 9}$, *Arl8b*$^{\Delta 9/\Delta 9}$ in *Arl8b*$^{\Delta 9}$ strain, respectively.
N = 6, 21 and 7 mice for *Arl8b*$^{+/+}$, *Arl8b*$^{+/Q75L}$ and *Arl8b*$^{Q75L/Q75L}$ strain, respectively.
N = 8, 11 and 4 mice for *Arl8b*$^{+/+}$, *Arl8b*$^{+/T34N}$ and *Arl8b*$^{T34N/T34N}$ in *Arl8b*^{T34N} strain, respectively. Error Bars represent s.e.m. *P < 0.05, **P < 0.01 (Bonferroni / Dunnet test).

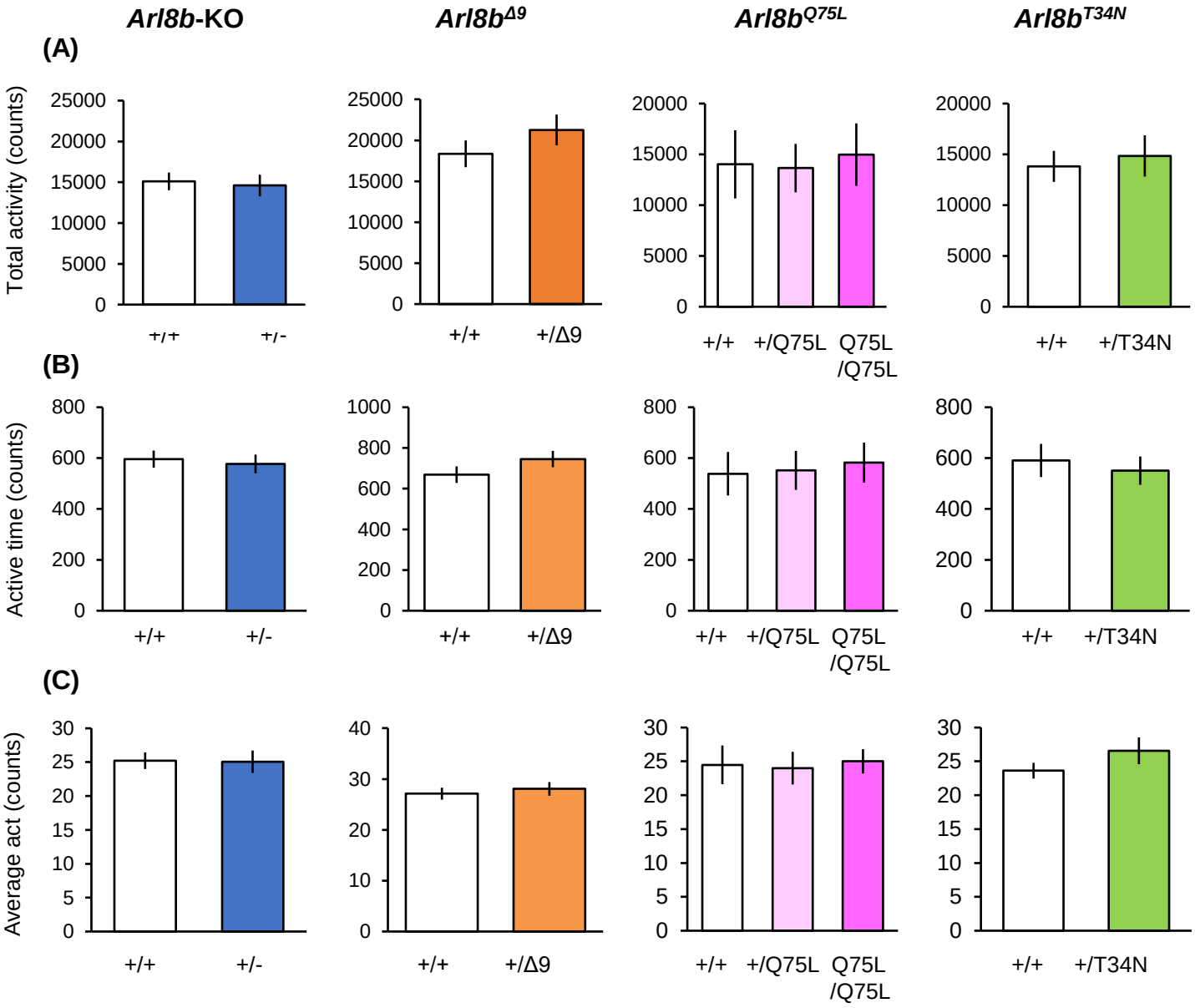

Figure 18. Comparison of home-cage activity in *Arl8b* gene-edited mice.
Total locomotor activity (A), active time (B) and average locomotor activity in the home-cage test were calculated in four *Arl8b* mutant strains.
N = 16 and 17 mice for $Arl8b^{+/+}$ and $Arl8b^{+/-}$ in *Arl8b*-KO strain, respectively.
N = 14 and 14 mice for $Arl8b^{+/+}$ and $Arl8b^{+/\Delta 9}$ in $Arl8b^{\Delta 9}$ strain, respectively.
N = 5, 8 and 4mice for $Arl8b^{+/+}$, $Arl8b^{+/Q75L}$ and $Arl8b^{Q75L/Q75L}$ strain, respectively.
N = 6 and 8 mice for $Arl8b^{+/+}$, $Arl8b^{+/T34N}$ *in* $Arl8b^{T34N}$ strain, respectively.
Error Bars represent s.e.m.

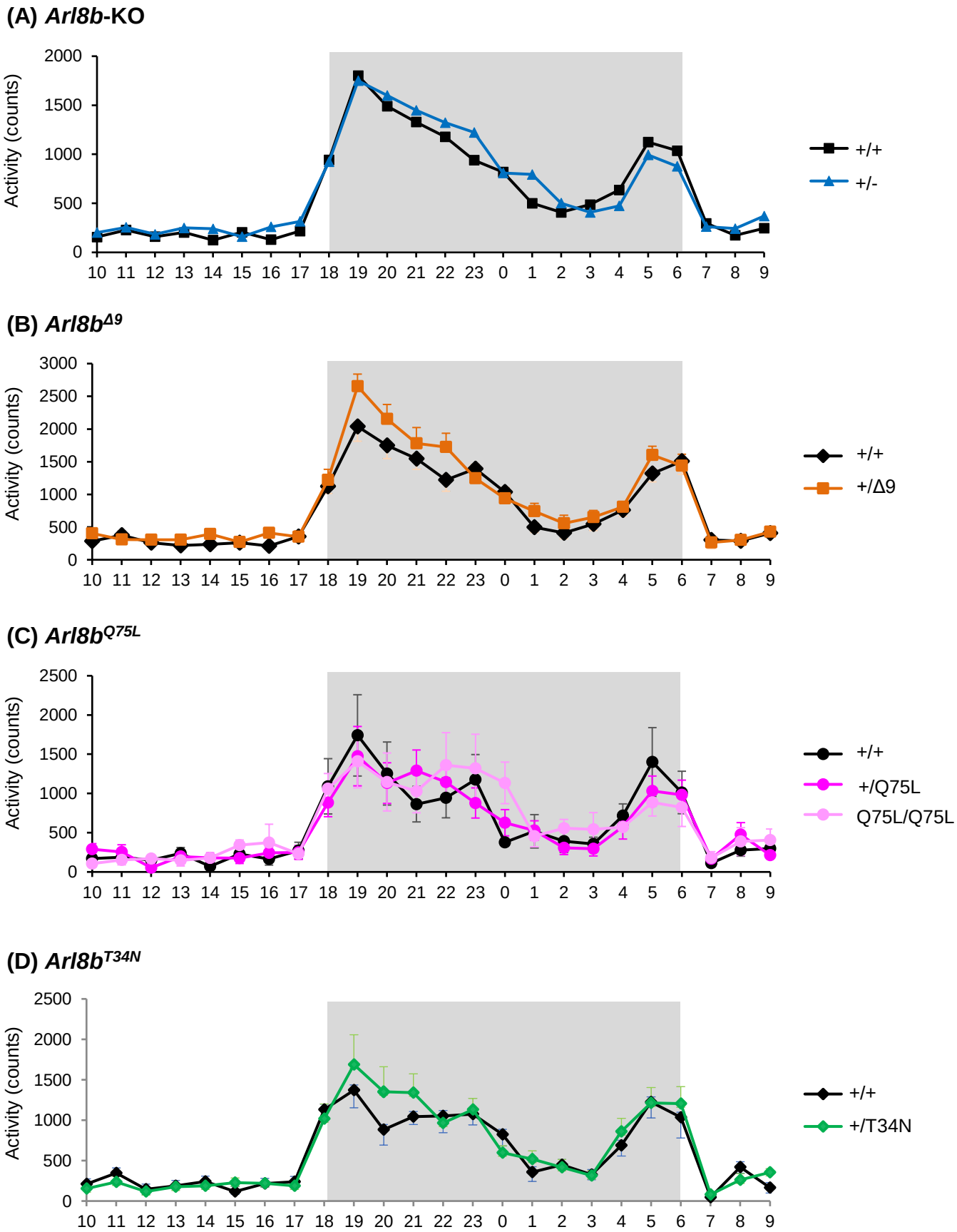

Figure 19. Temporal pattern of home-cage activity in *Arl8b*-KO (A), $Arl8b^{\Delta 9}$ (B), $Arl8b^{Q75L}$ (C) and $Arl8b^{T34N}$ (D). Dark phase is marked by gray background colors.
N = 16 and 17 mice for $Arl8b^{+/+}$ and $Arl8b^{+/-}$,respectively, in *Arl8b*-KO strain.
N = 14 and for each of $Arl8b^{+/+}$ and $Arl8b^{+/\Delta 9}$ in $Arl8b^{\Delta 9}$ strain.
N = 5, 8 and 4 mice for $Arl8b^{+/+}$, $Arl8b^{+/Q75L}$ and $Arl8b^{Q75L/Q75L}$ strain, respectively.
N = 6 and 8 mice for $Arl8b^{+/+}$ and $Arl8b^{+/T34N}$, respectively, in $Arl8b^{T34N}$ strain.
Error Bars represent s.e.m.

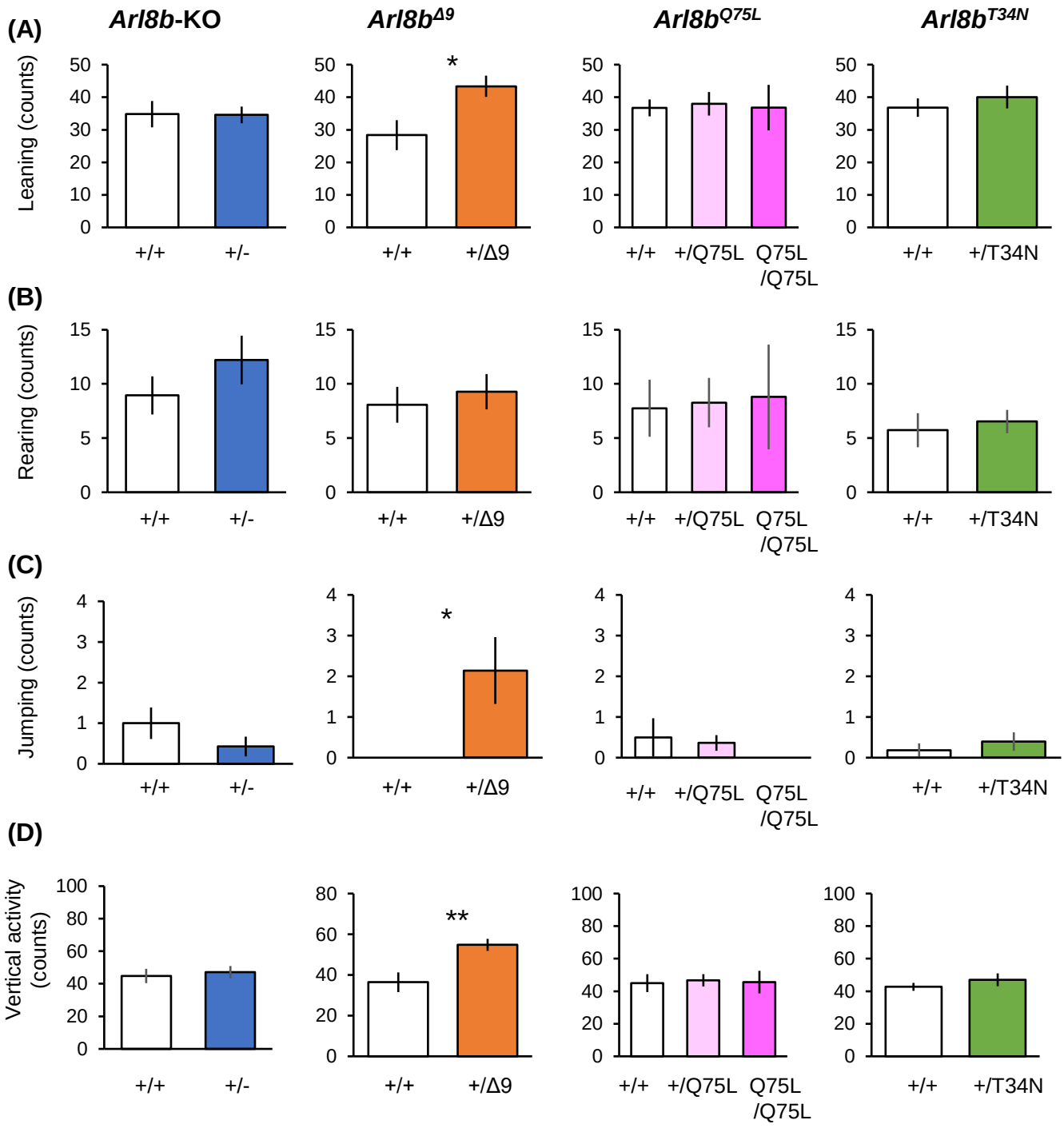

Figure 20. Behavioral components of the open field test in four Arl8b mutant strains: *Arl8b*-KO, $Arl8b^{\Delta 9}$, $Arl8b^{Q75L}$ and $Arl8b^{T34N}$.
The number of leaning (A), rearing (B), jumping (C) were calculated. Vertical activity (D) is the total number of learning, rearing and jumping.
N = 16 and 14 mice for $Arl8b^{+/+}$ and $Arl8b^{+/-}$, respectively, in *Arl8b*-KO strain.
N = 13 and 14 mice for $Arl8b^{+/+}$ and $Arl8b^{+/\Delta 9}$, respectively, in $Arl8b^{\Delta 9}$ strain.
N = 8, 11 and 6 mice for $Arl8b^{+/+}$, $Arl8b^{+/Q75L}$ and $Arl8b^{Q75L/Q75L}$ strain, respectively.
N = 11 and 15 mice for $Arl8b^{+/+}$ and $Arl8b^{+/T34N}$, respectively, in $Arl8b^{T34N}$ strain.
Error Bars represent s.e.m. *p < 0.05 (one-way, ANOVA).

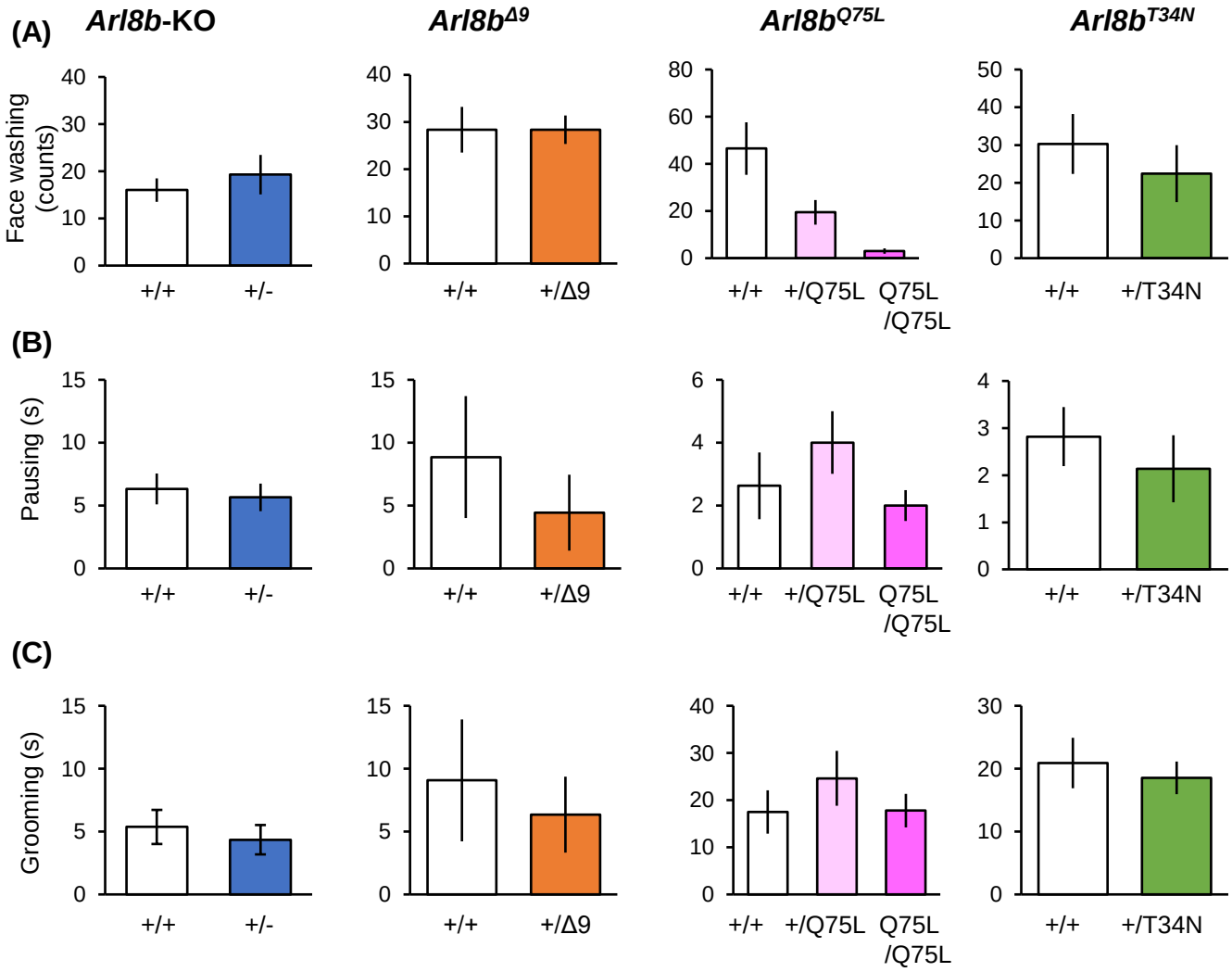

Figure 21. Behavioral components of the open field test in four Arl8b mutant strains: *Arl8b*-KO, *Arl8b*$^{\Delta 9}$, *Arl8b*^{Q75L} and *Arl8b*^{T34N} .
The number of face washing (A), pausing (B) and the duration of grooming (C) were calculated.
N = 16 and 14 mice for *Arl8b*$^{+/+}$ and *Arl8b*$^{+/-}$, respectively, in *Arl8b*-KO strain.
N = 13 and 14 mice for *Arl8b*$^{+/+}$ and *Arl8b*$^{+/\Delta 9}$, respectively, in *Arl8b*$^{\Delta 9}$ strain.
N = 8, 11 and 6 mice for *Arl8b*$^{+/+}$, *Arl8b*$^{+/Q75L}$ and *Arl8b*$^{Q75L/Q75L}$ strain, respectively.
N = 11 and 15 mice for *Arl8b*$^{+/+}$ and *Arl8b*$^{+/T34N}$ *in Arl8b*^{T34N} strain , respectively.
Error Bars represent s.e.m.

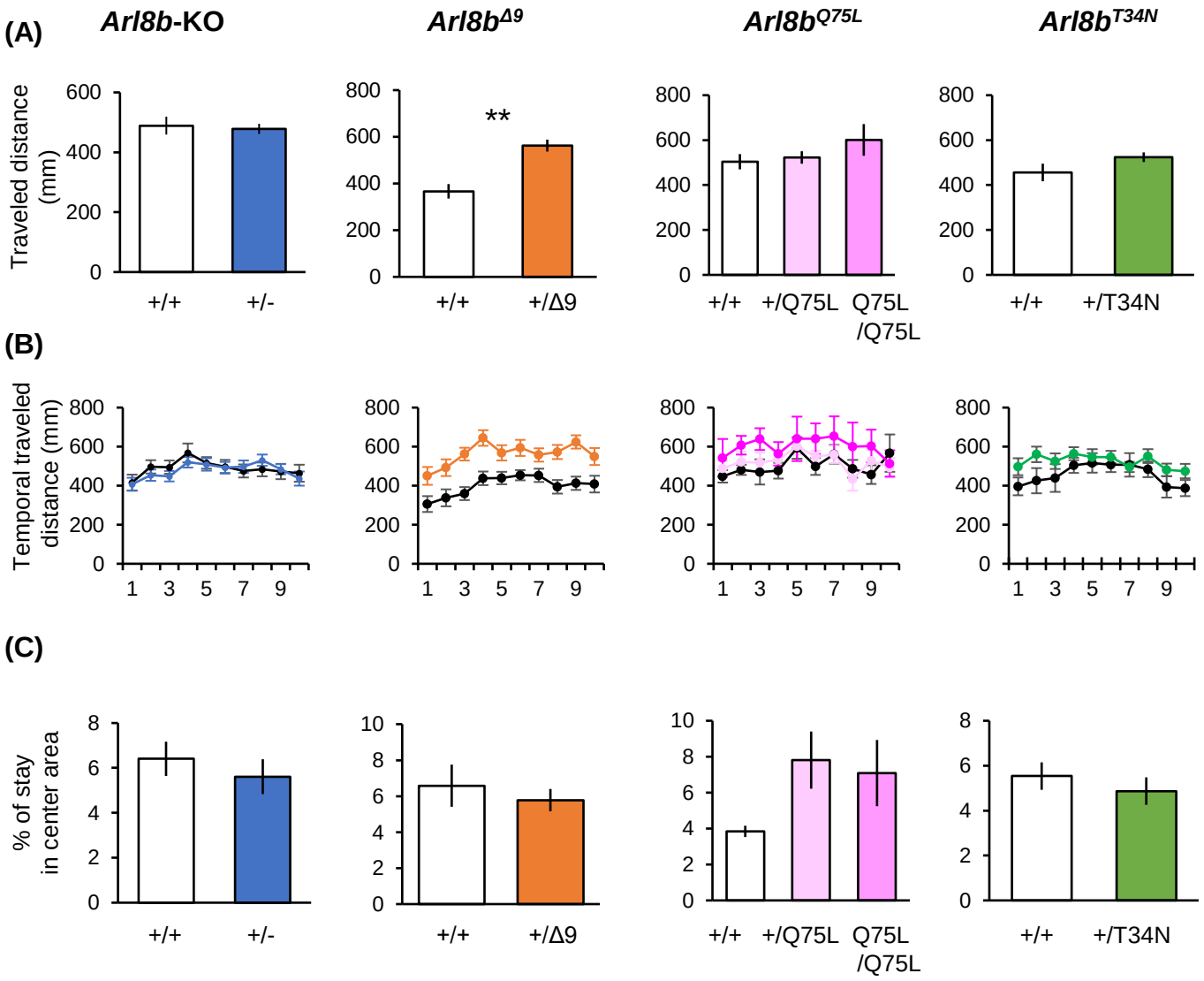

Figure 22. Open-field test in *Arl8b* gene-edited mice.
The average traveled distance (A), temporal traveled distance (B), and the percentage of staying time in the center of the arena (B) were recorded.
N = 16 and 14 mice for $Arl8b^{+/+}$ and $Arl8b^{+/-}$, respectively, in *Arl8b*-KO strain.
N = 13 and 14 mice for $Arl8b^{+/+}$ and $Arl8b^{+/\Delta 9}$, respectively, in $Arl8b^{\Delta 9}$ strain.
N = 8, 11 and 6 mice for $Arl8b^{+/+}$, $Arl8b^{+/Q75L}$ and $Arl8b^{Q75L/Q75L}$ strain, respectively,.
N = 11 and 15 mice for $Arl8b^{+/+}$ and $Arl8b^{+/T34N}$, respectively, in $Arl8b^{T34N}$ strain.
Error Bars represent s.e.m. **p < 0.01 (one-way ANOVA).

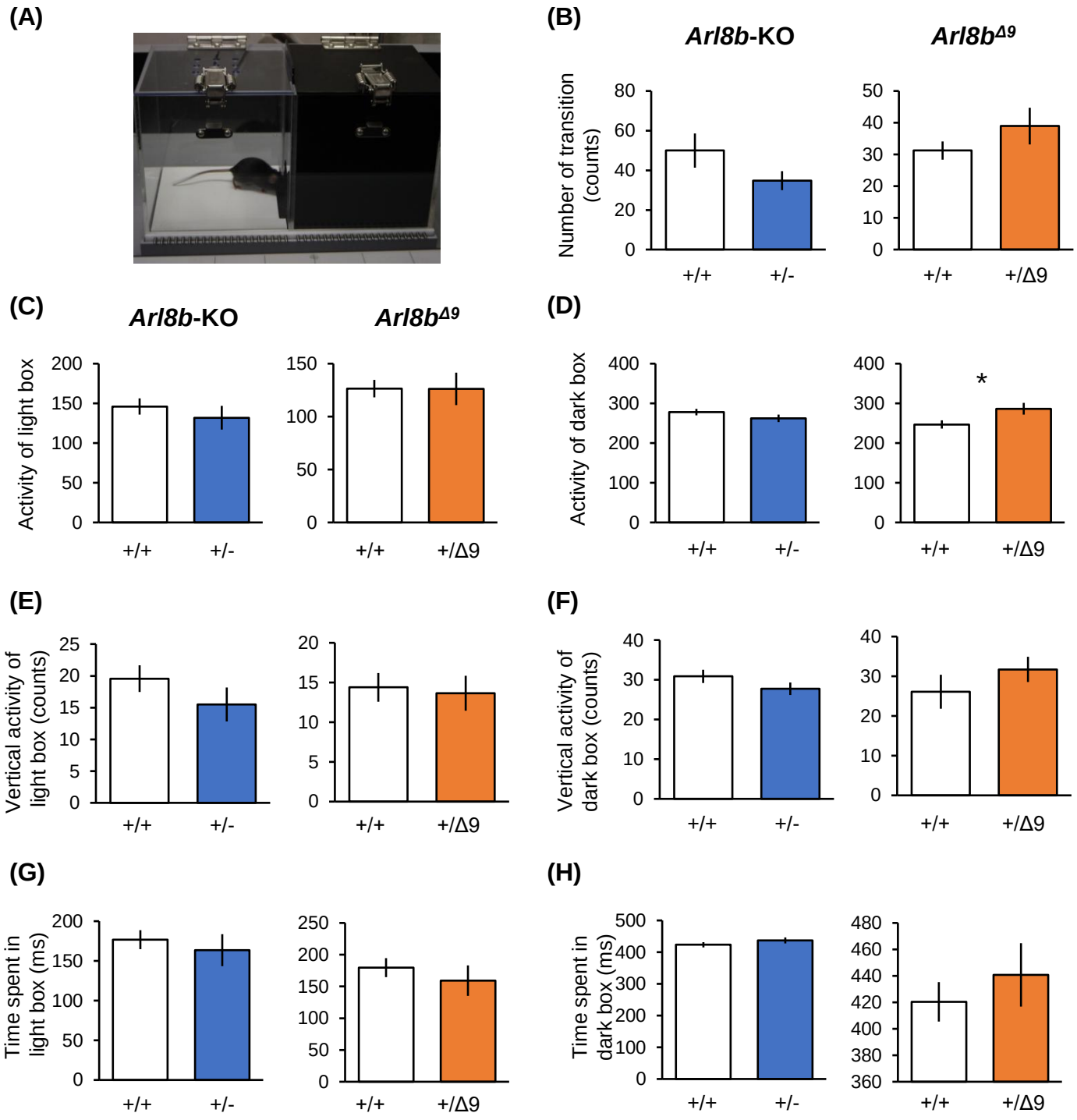

Figure 23. Light and dark box test of *Arl8b*-KO, *Arl8b*$^{\Delta 9}$ strain.
(A) The apparatus of the light and dark box test. The number of transition between the light and the dark box (B) was calculated. Activity of the light (C) and the dark box (D), vertical activity of the light (E) and the dark box (F) were also scored. Time spent in the light (G) and the dark box (H) were measured .
N = 13 and 12 mice for *Arl8b*$^{+/+}$ and *Arl8b*$^{+/-}$, respectively, in *Arl8b*-KO strain.
N = 13 and 14 mice for *Arl8b*$^{+/+}$ and *Arl8b*$^{+/\Delta 9}$, respectively, in *Arl8b*$^{\Delta 9}$ strain.
Error Bars represent SEM;*p < 0.05 (one-way ANOVA).

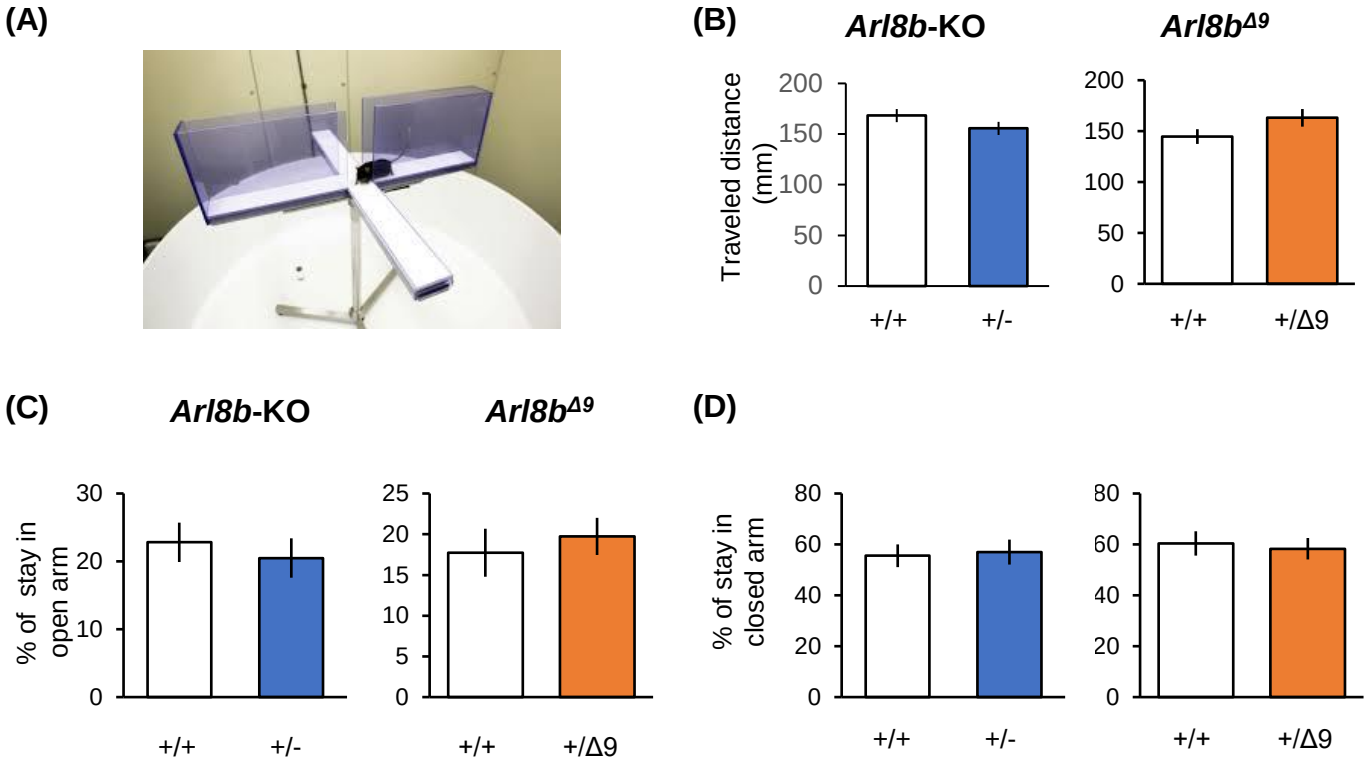

Figure 24. Elevated plus maze test of *Arl8b*-KO, *Arl8b*$^{\Delta 9}$ strain.
(A)The apparatus of the elevated plus maze test. Traveled distance (B), the percentage of the time spent in the open arm (C) and the closed arm (D) were measured.
N = 13 and 12 mice for *Arl8b*$^{+/+}$ and *Arl8b*$^{+/-}$, respectively, in *Arl8b*-KO strain.
N = 13 and 14 mice for *Arl8b*$^{+/+}$ and *Arl8b*$^{+/\Delta 9}$, respectively, in *Arl8b*$^{\Delta 9}$ strain.
Error Bars represent SEM;**p < 0.01
.

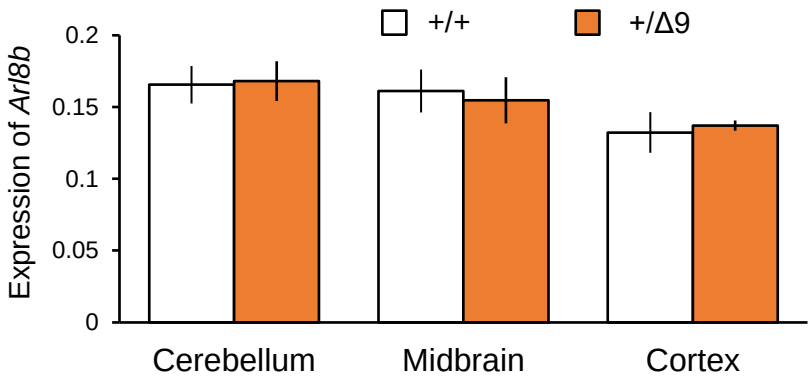

Figure 25. Expression of *Arl8b* in brain tissues in *Arl8b*$^{\Delta 9}$ mice.
Expression was assessed by qRT-PCR, normalizing to β-actin. Relative mRNA expression of *Arl8b* in cerebellum, midbrain and cortex of *Arl8b*$^{+/+}$ (+/+) and *Arl8b*$^{+/\Delta 9bp}$ (+/Δ9) mice . N = 5 for each mouse strain. Error Bars represent s.e.m.